

# Arrested kinetic Li isotope fractionation at the margin of the Ilímaussaq complex, South Greenland: Evidence for open-system processes during final cooling of peralkaline igneous rocks <sup>☆</sup>

Michael A.W. Marks <sup>a,\*</sup>, Roberta L. Rudnick <sup>b</sup>, Catherine McCammon <sup>c</sup>,  
Torsten Vennemann <sup>d</sup>, Gregor Markl <sup>a</sup>

<sup>a</sup> Institut für Geowissenschaften, AB Mineralogie und Geodynamik, Eberhard-Karls-Universität, Wilhelmstraße 56, D-72074 Tübingen, Germany

<sup>b</sup> Geochemistry Laboratory, Department of Geology, University of Maryland, College Park, MD 20742, USA

<sup>c</sup> Bayerisches Geoinstitut, Universität Bayreuth, D-95440 Bayreuth, Germany

<sup>d</sup> Institut de Minéralogie et Géochimie, Université de Lausanne, L'Anthropole, CH-1015 Lausanne, Switzerland

Received 16 May 2007; received in revised form 1 October 2007; accepted 3 October 2007

Editor: S.L. Goldstein

## Abstract

Li contents [Li] and isotopic composition ( $\delta^7\text{Li}$ ) of mafic minerals (mainly amphibole and clinopyroxene) from the alkaline to peralkaline Ilímaussaq plutonic complex, South Greenland, track the behavior of Li and its isotopes during magmatic differentiation and final cooling of an alkaline igneous system. [Li] in amphibole increase from <10 ppm in Ca-amphiboles of the least differentiated unit to >3000 ppm in Na-amphiboles of the highly evolved units. In contrast, [Li] in clinopyroxene are comparatively low (<85 ppm) and do not vary systematically with differentiation. The distribution of Li between amphibole and pyroxene is controlled by the major element composition of the minerals (Ca-rich and Na-rich, respectively) and changes in oxygen fugacity (due to Li incorporation via coupled substitution with ferric iron) during magmatic differentiation.

$\delta^7\text{Li}$  values of all minerals span a wide range from +17 to –8‰, with the different intrusive units of the complex having distinct Li isotopic systematics. Amphiboles, which dominate the Li budget of whole-rocks from the inner part of the complex, have constant  $\delta^7\text{Li}$  of  $+1.8 \pm 2.2\%$  ( $2\sigma$ ,  $n=15$ ). This value reflects a homogeneous melt reservoir and is consistent with their mantle derivation, in agreement with published O and Nd isotopic data. Clinopyroxenes of these samples are consistently lighter, with  $\Delta^7\text{Li}_{\text{amph-cpx}}$  as large as 8‰ and are thus not in Li isotope equilibrium. These low values probably reflect late-stage diffusion of Li into clinopyroxene during final cooling of the rocks, thus enriching the clinopyroxene in  $^6\text{Li}$ .

At the margin of the complex  $\delta^7\text{Li}$  in the syenites increases systematically, from +2 to high values of +14‰. This, coupled with the observed Li isotope systematics of the granitic country rocks, reflects post-magmatic open-system processes occurring during final cooling of the intrusion. Although the shape and magnitude of the Li isotope and elemental profiles through syenite and country rock are suggestive of diffusion-driven isotope fractionation, they cannot be modeled by one-dimensional diffusive transport and point to circulation of a fluid having a high  $\delta^7\text{Li}$  value (possibly seawater) along the chilled contact. In all, this study

<sup>☆</sup> Contribution to the mineralogy of Ilímaussaq No. 132.

\* Corresponding author.

E-mail address: [michael.marks@uni-tuebingen.de](mailto:michael.marks@uni-tuebingen.de) (M.A.W. Marks).

demonstrates that Li isotopes can be used to identify complex fluid- and diffusion-governed processes taking place during the final cooling of such rocks.

© 2007 Elsevier B.V. All rights reserved.

*Keywords:* Ilímaussaq; Li isotopes; Kinetic fractionation; Peralkaline igneous rock

## 1. Introduction

Li generally behaves as a moderately incompatible element during igneous fractionation (Ryan and Langmuir, 1987; Brenan et al., 1998a). Consequently, exceptional enrichments in Li occur in highly fractionated rocks such as peraluminous leucogranites (e.g., Badanina et al., 2004), granitic pegmatites (e.g., Cerny et al., 2005; Teng et al., 2006a) and peralkaline nepheline syenites (e.g., Schmitt et al., 2000; Bailey et al., 2001).

Unlike many incompatible trace elements, experimental and empirical studies have shown that Li preferentially partitions into an aqueous fluid phase during mineral–fluid equilibria (e.g., Chan et al., 1994; You et al., 1994; You and Chan, 1996; Brenan et al., 1998b). Thus, Li is fluid-mobile and can be transported during magmatic alteration, magmatic fluid exsolution and hydrothermal circulation (e.g., Berger et al., 1988; Seyfried et al., 1998; Brenan et al., 1998b; Audétat and Pettke, 2003).

The large mass difference (about 17%) between the two stable isotopes,  $^6\text{Li}$  and  $^7\text{Li}$ , results in a large natural variation of Li isotopes of about 80‰ (e.g., Rudnick & Nakamura, 2004; Tomascak, 2004 and references therein). Processes leading to extensive fractionation of Li isotopes documented so far include low-temperature fluid–rock interaction (e.g., Chan et al., 1992; Huh et al., 1998; Huh et al., 2001; Decitre et al., 2002; James et al., 2003; Pistiner and Henderson, 2003; Rudnick et al., 2004; Benton et al., 2004), metamorphic dehydration of basalts (Zack et al., 2003) and Li diffusion (e.g., Richter et al., 2003; Lundstrom et al., 2005; Teng et al., 2006a; Rudnick & Ionov, 2007; Jeffcoate et al., 2007; Parkinson et al., 2007). High-temperature magmatic differentiation does not produce significant fractionation of Li isotopes (e.g., Tomascak et al., 1999a; Bryant et al., 2004; Teng et al., 2004a). Moreover, Halama et al. (2007) demonstrated no fractionation of Li isotopes in carbonatite magmas down to very low temperatures (500 °C). However, recent experiments indicate that resolvable Li isotope fractionation may occur between minerals and coexisting fluid at magmatic temperatures (Lynton et al., 2005; Wunder et al., 2006, 2007). The experimental

results of Wunder et al. are corroborated by studies of pegmatites that demonstrate isotopic fractionation of several permil during very high degrees of crystal fractionation and fluid–melt equilibration at  $T \leq 350$  °C (Teng et al., 2006b). To date, however, documentation of Li isotope behavior during magmatic differentiation is still limited and a fuller understanding may be had by studies of igneous rocks of more diverse compositions.

This study reports the Li concentrations and isotopic compositions of mafic minerals (amphibole, clinopyroxene and biotite) and some whole-rocks from the peralkaline Ilímaussaq plutonic complex, South Greenland, and its surrounding country rocks. The geology, geochemistry, mineral chemistry and petrology of the complex are known in great detail (Sørensen, 2001 and references therein), thus providing an excellent background against which the behavior of Li isotopes within a single alkaline plutonic complex can be investigated. Since differentiation occurred over an extensive temperature range (1000 to 300 °C), including orthomagmatic and late-stage hydrothermal crystallization, the Ilímaussaq suite can offer detailed insights into the behavior of Li isotopes during magmatic differentiation, fluid exsolution and final cooling of a peralkaline igneous system.

## 2. Geological framework and previous work

The 1.16 Ga old (Blaxland, 1976; Krumrei et al., 2006) Ilímaussaq intrusion (Fig. 1) is one of ten major alkaline intrusions in the Mid-Proterozoic rift-related Gardar Province of South Greenland. It intrudes Early-Proterozoic I-type granitoids (the 1.80–1.85 Ga Julia-nehåb batholith; Kalsbeek and Taylor, 1985; Garde et al., 2002) and a sequence of basalts and interlayered sedimentary rocks (Eriksfjord Formation; Poulsen, 1964; Halama et al., 2003). The Ilímaussaq complex is the type locality for agpaite rocks, which are peralkaline nepheline syenites containing complex Na-(Ti, Zr)-silicates (e.g., eudialyte; Sørensen, 1997). Based on indicators of differentiation in whole-rocks and minerals (e.g., Fe/Mg, (Na+K)/Al, Ca/(Na+K), Rb/Sr, Mg/Li), Ilímaussaq is the most differentiated alkaline igneous

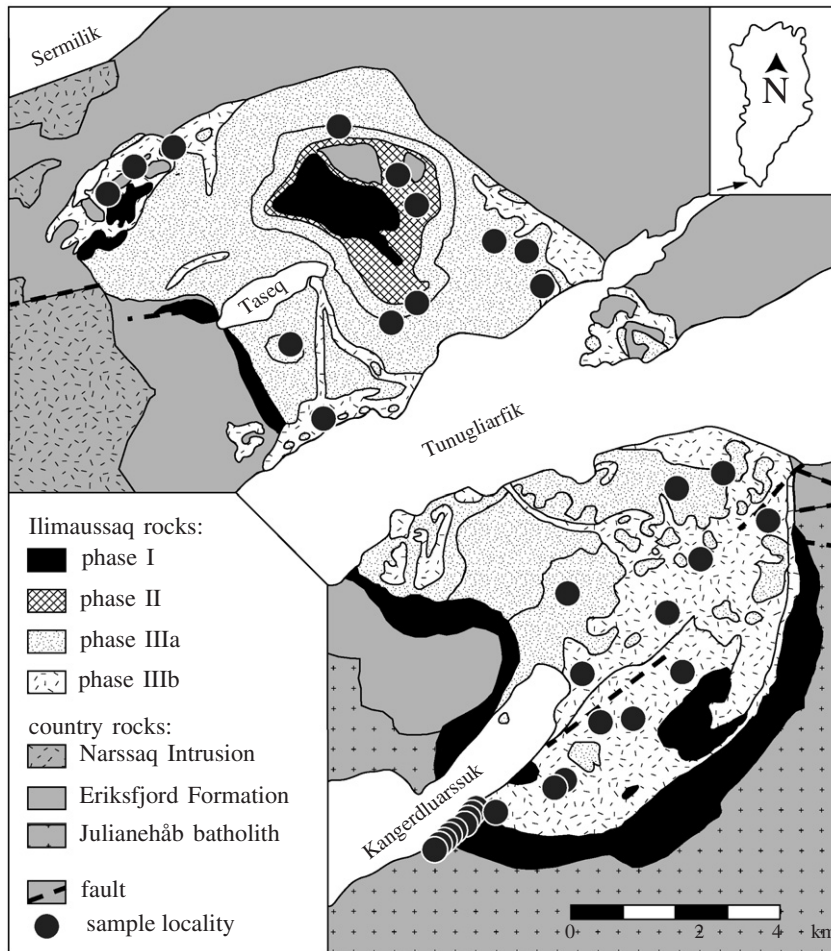


Fig. 1. Geological sketch map of the Ilímaussaq complex with sample localities, modified after Ferguson (1964).

rock suite yet documented (Bailey et al., 2001; Sørensen, 2001).

The complex formed from four melt batches (Sørensen, 2006), which intruded successively at 3–4 km depth (0.1 GPa). The earliest melt batch consists of an alkaline, augite syenite (phase I), which was later intruded by a peralkaline granite (phase II). Phases IIIa and IIIb comprise the bulk of the complex and consist of a sequence of highly fractionated apaitic nepheline syenites (pulaskite, sodalite foyaite, naujiaite, kakortokite, and lujavrite). Abundant pegmatites and hydrothermal veins occur in all rock units; the latter are also found in the granite country rocks (Ranløv and Dymek, 1991 and our own observations), reflecting intensive hydrothermal activity during the final stages of cooling (e.g., Engell et al., 1971; Markl and Baumgartner, 2002).

The Ilímaussaq rocks are interpreted to be derived from a single parental alkali basaltic magma that

fractionated in a deep-seated magma chamber in a continental rift setting (Larsen and Sørensen, 1987; Stevenson et al., 1997). Relatively homogeneous neodymium ( $\epsilon_{Nd} = -0.9$  to  $-1.8$ ) and oxygen isotope compositions ( $\delta^{18}O_{V-SMOW} = 5.2$  to  $5.7\%$ ) of mafic minerals from the major rock types indicate that most of the Ilímaussaq melts are derived from an isotopically homogeneous OIB-type mantle source, with generally no evidence for subsequent crustal contamination (Marks et al., 2004). The only exception is the peralkaline granite, which has lower  $\epsilon_{Nd}$  ( $-3.1$ ) that is interpreted to reflect contamination with lower crustal rocks (Marks et al., 2004).

Overall, the Ilímaussaq rocks record a prolonged crystallization interval between about  $1000^{\circ}$  and  $300^{\circ}$  C, including late-stage hydrothermal activity (Larsen, 1976; Markl, 2001; Markl et al., 2001; Marks and Markl, 2001; Marks et al., 2004). Low oxygen fugacity of the parental melt resulted in highly reduced phase

Table 1

Mineral assemblages and information on equilibration conditions for the major Ilímaussaq rocks (after Markl et al., 2001; Marks et al., 2003)

	Phase I	Phase II	Phase III			
	Augite syenite	Peralkaline granite	IIIa		IIIb	
			Sodalite foyaite	Naujaite	Kakortokite	Lujavrite
Magmatic to late-magmatic phases	Alkfsp, Ne, Ol, Aug, Ap, Mag, Ilm, Amph, Bt	Alkfsp, Qtz, Amph, Aeg	Alkfsp, Ne, Aeg, So, Ap, Ol, Amph, Aen, Eud, Bt, Anl	Sod, Ne, Fl, Ap, Sph, Alkfsp, Amph, Aeg, Eud, Ne, Aen, Pct	Alkfsp, Sod, Ne, Eud, Ap, Amph, Aeg, Fl, Anl, Bt	Aeg, Amph, Eud, Ab, Mic, Sod, Ne+rare specialities like neptunite etc.
Sub-solidus and hydrothermal phases	Sod, Anl, Ms, Hgrs, Sph, Gal, Ccp	Aeg, Astr	Sod, Anl, Ab, Ntr, Aeg	Ntr, Anl, Sod	Anl, Aeg, Ab	Aeg, Ntr, Sod, Anl, Uss, Vil
Near-liquidus conditions	≈ 1000 °C (fsp)	≥ 750 °C	≈ 950 °C (ne)			≈ 850 °C (ne)
Near-solidus conditions	800–650 °C (QUILF) ≈ 600 °C (bt)		≈ 550 °C (ne–jd–ab)			≈ 500 °C (ne–jd–ab)
Hydrothermal alteration	≈ 400 °C (sod–anl)	≤ 350 °C (aeg–arf)	≈ 400 °C (anl–sod)			≈ 350 °C (ne–jd–ab)
Samples used in the present study	GM1857, GM1858, GM1330, GM1332, GM1333	GM1303, ILM154	GM1214, GM1219	GM1369, GM1370	GM1334, GM1335, GM1337, XL61, XL63	GM1843, GM1294, GM1272, ILM157, ILM145

The location of the Ilímaussaq complex is 60°56' N and 45°56' W (using Google Earth).

assemblages (e.g., Ti-rich magnetite; Marks and Markl, 2001) and caused the formation of two immiscible magmatic fluids, which were present during most of the crystallization history: a methane-dominated vapor phase and a highly saline aqueous fluid phase (e.g., Konnerup-Madsen, 2001; Markl et al., 2001; Krumrei et al., 2007). Extremely low  $\delta D$  values of amphiboles from the agpaite rocks ( $\delta D = -132$  to  $-232\text{‰}$ ) are interpreted to have resulted from H-isotope re-equilibration between amphiboles and internally generated, D-depleted fluids formed by late-stage oxidation of an earlier CH<sub>4</sub>-dominated magmatic vapor phase (Marks et al., 2004).

Amphibole and clinopyroxene are abundant and well-preserved in most Ilímaussaq rocks and are thus well suited for a Li isotope study of magmatic processes. Amphibole compositions evolve from Ca-amphibole in the augite syenite via Na–Ca amphibole to Na-amphibole in the agpaite rocks. Similarly, clinopyroxene evolves from augitic compositions towards near end-member aegirine (Larsen 1976; Markl et al., 2001; Marks et al., 2004).

### 3. Samples

More than sixty mineral separates and whole-rocks from representative samples of the major rock types, late-stage pegmatites and hydrothermal veins from the Ilímaussaq complex were analyzed along with nineteen

whole-rock samples of country rocks (granites, basalts, sandstones). Table 1 gives an overview of the mineral assemblages of the major Ilímaussaq rocks along with information on their estimated equilibration conditions (Markl et al., 2001; Marks and Markl, 2001). The Ilímaussaq rocks typically have a prolonged crystallization interval and experienced a late-stage hydrothermal alteration, which overprinted or replaced the primary mineral assemblages (Markl et al., 2001, see below). Where possible, primary igneous amphibole and clinopyroxene (and biotite in augite syenites) have been analyzed. In samples for which only amphibole or clinopyroxene data are presented, the missing mineral was either not present or was present in only very low abundance. Most of the samples analyzed here have been subject to previous petrological and geochemical investigations (Markl, 2001; Markl et al., 2001; Marks and Markl, 2001; Markl and Baumgartner, 2002; Marks et al., 2004) and thus, only brief descriptions of sample localities and the relationships between samples are provided here.

From the augite syenite unit (phase I), five samples were analyzed from traverse AS3 of Marks and Markl (2001), extending over ≈ 600 m from the outer chilled contact with granitic country rocks towards the inner contact with the agpaite rocks (Fig. 1). Intrinsic parameters ( $T$ ,  $a_{\text{SiO}_2}$ ,  $f_{\text{O}_2}$ ) as well as mineral compositions ( $X_{\text{Fe}}$ , Ca/Na) change systematically across this traverse, reflecting increasing differentiation towards

the contact with the agpaite rocks (Marks and Markl, 2001). Ternary feldspar crystallized at  $\approx 1000$  °C on the liquidus, followed by magnetite, olivine and augite at 800–650 °C, late-magmatic amphibole and biotite formed at 700–600 °C and analcite–sodalite–hydrogrossular assemblages disseminated in some samples reflect hydrothermal alteration at  $\approx 400$  °C (Marks and Markl, 2001; Markl et al., 2001).

Two samples were analyzed from the peralkaline granite (phase II). Due to the lack of appropriate mineral assemblages, no detailed equilibration conditions for this unit can be estimated, however, by analogy with similar occurrences in the Gardar Province, the granite probably crystallized at  $\geq 750$  °C (Marks et al., 2003). The formation of aegirine at the expense of arfvedsonite in such rock types was shown to be a late-stage process, possibly occurring at temperatures  $\leq 350$  °C (Marks et al., 2003).

From phases IIIa and IIIb, fifteen samples were analyzed: one pulaskite, two sodalite foyaites, two naujaite, five kakortokites, and five lujavrites. Nepheline thermometry of early nepheline indicates near-liquidus temperatures of  $\approx 950$ –850 °C and near-solidus conditions of 550–500 °C are indicated by activities of late nepheline, albite and jadeite (components in nepheline solid solution, alkali feldspar and clinopyroxene, respectively). Hydrothermal alteration at 400–350 °C is indicated by the late-stage assemblages of albite, nepheline, analcite, sodalite and aegirine (Markl et al., 2001; Markl and Baumgartner, 2002).

Three different pegmatites were analyzed for this study. They consist primarily of microcline+arfvedsonite±aegirine±eudialyte and are believed to have formed either from very late-stage melts or fluid–melt mixtures (Markl and Baumgartner, 2002). One late-stage dyke rock (GM1212) was also analyzed. This rock shows evidence of having formed by liquid immiscibility at temperatures of 600–500 °C (Markl, 2001). Seven hydrothermal veins cutting different phase III rocks were selected for analyses: one albite-rich arfvedsonite-bearing aplitic rock (ILM101), one arfvedsonite–sodalite-dominated vein (GM1246), one albite-rich, arfvedsonite- and tugtupite (Na-Be-silicate)-bearing vein (GG02), one zoned vein with aegirine-rich rims and an arfvedsonite-rich center (ILM124), and three aegirine–albite veins (GM1257 and ILM165). Additionally, one aegirine vein (ILM192) cutting the basement granite some 250 m outside the Ilímaussaq complex was analyzed. The hydrothermal veins crystallized at 500–300 °C from late-magmatic fluids or supercritical fluid–melt-mixtures (Markl and Baumgartner, 2002).

A total of nineteen country rocks (granites, basalts and sandstones) from the vicinity of the Ilímaussaq complex were analyzed. Some of these were studied by Halama et al. (2003, 2004). Three volcanic as well as two sedimentary rocks were analyzed from the Eriksfjord Formation. One additional sample is from a several 100 m quartzite xenolith from within the augite syenite. Thirteen basement granite samples were analyzed. Four of them (BT 3, BT 5, BT 6, JG 2) were collected several km's away from the Ilímaussaq complex, whereas nine samples (JG 5–JG 13) were collected along the extension of the augite syenite sampling traverse at distances between 0.2 and 225 m away from the contact. Whereas most granite samples are typical two feldspar-granites with quartz, biotite and minor magnetite, granites sampled within 45 m of the augite syenite show secondary sodic pyroxene or sodic amphibole. Feldspar in these samples is extremely cloudy and is converted into a chess-board variety of microcline. It is assumed that these features result from post-magmatic interaction with an alkaline fluid phase expelled from the Ilímaussaq complex.

#### 4. Analytical methods

Mineral separates were hand picked to optical purity and cleaned in Milli-Q® water (18.2 M $\Omega$  cm) three times, for 15 min per wash. Li isotope analyses were carried out at the University of Maryland and full details are provided in Rudnick et al. (2004) and Teng et al. (2006b). In order to monitor the Li yield, before and after cuts (2 ml each) were analyzed for their Li content using an Element 2, single collector ICP-MS (see below). The total Li procedural blank is  $\sim 250$  pg Li and has a  $\delta^7\text{Li}$  value of  $-45\%$ . This blank is negligible compared to the amount of Li processed for the samples (generally  $> 50$  ng), and a precision of  $\pm 1\%$  ( $2\sigma$ ). Thus, no blank correction was made.

All Li isotope results are reported in the  $\delta^7\text{Li}$  notation with  $\delta^7\text{Li} = 1000 \cdot [{}^7\text{Li}/{}^6\text{Li}_{\text{sample}}/{}^7\text{Li}/{}^6\text{Li}_{\text{standard}} - 1]$  relative to the L-SVEC standard (Flesch et al., 1973) and are calculated by comparison of the unknown sample to the average of the two bracketing standard analyses, as described in Tomascak et al. (1999b). Analyses consist of two blocks of 20 ratios each, yielding an in-run precision of  ${}^7\text{Li}/{}^6\text{Li}$  measurements is generally  $\pm 0.2\%$  or better, with no systematic change in the  ${}^7\text{Li}/{}^6\text{Li}$  ratio. The external precision, based on repeat analyses of Li standard solutions, is  $\pm 1\%$  ( $2\sigma$ ) or better. For example, pure Li solutions (UMD-1 and IRMM-016) gave  $\delta^7\text{Li}$  values of  $+54.5 \pm 0.5\%$  ( $2\sigma$ ,  $n=26$ ) and  $-0.8 \pm 0.4\%$  ( $2\sigma$ ,  $n=14$ ), respectively, values falling in previously

Table 2a

Li concentration, Li, O and H isotope data, Li yield from column chemistry and  $D_{\text{amph-cpx}}$  values of mineral separates and whole-rock samples from the augite syenite unit (phase 1) along with their distance to the granitic basement

Sample	Distance to basement rocks (m)	Amphibole						Clinopyroxene				$\Delta^7\text{Li}$ (amph-cpx) (‰)	$D_{\text{amph-cpx}}$	$\Delta^{18}\text{O}$ (amph-cpx) (‰)	Biotite				Whole-rock			
		[Li] (ppm)	$\delta^7\text{Li}$ (‰)	Li yield (%)	$\delta^{18}\text{O}$ (‰)	$\delta D$ (‰)	$\text{Fe}^{3+}/\Sigma\text{Fe}$	[Li] (ppm)	$\delta^7\text{Li}$ (‰)	Li yield (%)	$\delta^{18}\text{O}$ (‰)				[Li] (ppm)	$\delta^7\text{Li}$ (‰)	Li yield (%)	$\delta^{18}\text{O}$ (‰)	[Li] (ppm)	$\delta^7\text{Li}$ (‰)	Li yield (%)	$\delta^{18}\text{O}$ (‰)
GM 1858 <sup>1</sup>	2	7	+17.8	98.5	5.5	-78	0.08	14	+14.9	99.7	5.8	+1.9	0.5	-0.3	97	+16.8	99.6	-71	7.1	13.9	97.7	
		7	+16.9	97.7				15	+16.0	99.5					93	+17.4	99.6					
GM 1330	~150	56	+11.9	99.4	5.7*	-92*		39	+8.6	99.4	5.6*	+3.9	1.4	+0.1	195	+9.7	99.0	-86	23.1	11.6	95.3	6.7**
		51	+12.5	99.8				39	+7.9	99.7					184	+10.1	98.6					
GM 1332	~300	50	+5.9	98.6	5.2	-90		31	+6.3	94.0	5.8	-0.2	1.7	-0.6	-	+1.4	99.6	-83				
		61	+6.5	99.8				33	+6.3	98.5					227	+1.7	99.6					
GM 1333	~450	21	+0.3	99.3	5.4	-80		18	+6.0	98.6	5.6	-5.7	1.2	-0.2	Absent				25.5	1.7	98.5	
GM 1857 <sup>2</sup>	~600	64	+0.8	98.2	5.4	-101	0.12	51	+2.5	98.8	5.8	-1.9	1.4	-0.4	204	-1.3	99.5	-85	24.8	2.4	97.6	6.4**
		72	+0.6	98.9				49	+2.7	99.2					194	+0.4	99.8					

<sup>1</sup>=sample GM 1331 of Marks & Markl (2001); <sup>2</sup>=sample GM 1333\* of Marks & Markl (2001); \*=data from Marks et al. (2004); \*\*=data from Graser & Markl (in revision).  $\text{Fe}^{3+}/\Sigma\text{Fe}$  values are based on Mössbauer spectrometry.

Table 2b

Li concentration, Li, O and H isotope data, Li yield from column chemistry and  $D_{\text{amph-cpx}}$  values for mineral separates of the peralkaline granite (phase II), the apatitic rocks (phases IIIa and IIIb) and late-stage samples

Sample	Rock type	Amphibole						Clinopyroxene				$\Delta^7\text{Li}$ (amph-cpx) (‰)	$D_{\text{amph-cpx}}$	$\Delta^{18}\text{O}$ (amph-cpx) (‰)
		Li (ppm)	$\delta^7\text{Li}$ (‰)	Li yield (%)	$\delta^{18}\text{O}$ (‰)	$\delta D$ (‰)	$\text{Fe}^{3+}/\Sigma\text{Fe}$	Li (ppm)	$\delta^7\text{Li}$ (‰)	Li yield (%)	$\delta^{18}\text{O}$ (‰)			
<i>Phase II</i>														
GM1303	Peralk. granite replicate	579	+8.7 # +8.9	#	5.6*	-193*	0.23	Absent	-	-	-			
ILM154	Peralk. granite Replicate 1	431	+7.6	97.5				47	(+9.2)	95.7	3.1	+0.1	8.5	+2.3
	Replicate 2				5.4	-187	0.22	50	+7.4	98.2				
								51	+7.5	98.2				
<i>Phase IIIa</i>														
P-3-5	Pulaskite	364	+1.5	98.4			0.25	36	-3.8	98.6		+5.3	10.1	-
GM1214	Sodalite foyaite	644	+1.5	95.4	5.7*	-150*	0.23	33	-7.1	97.5	5.4	+8.3	18.8	+0.3
	Replicate 1	666	+1.4	97.1				35	-6.5	97.5				
	Replicate 2							36	-6.9	99.4				
GM1219	Sodalite foyaite	708	+2.1	99.9		-173	0.22	42	-4.4	97.3		+7.1	16.8	-
	Replicate	635	+1.2	97.9				38	-6.3	95.0				
GM1369	Naujaite	955	+2.1	96.4		-184	0.24	38	-3.2	99.2		+5.0	22.9	-
	Replicate 1	826	+1.7	97.9				40	-3.2	98.2				
	Replicate 2	898	+1.5	99.9										
GM1370	Naujaite	943	(+2.3)	92.2	5.4*	-198*	0.23	49	-3.4	99.3	5.0	+5.2	18.9	+0.4
	Replicate 1	931	+1.4	97.4				-	-3.8	99.4				
	Replicate 2	926	+1.8	99.1										
<i>Phase IIIb</i>														
GM1334	Kakortokite	649	+3.8	97.9		-192	0.25	43	-2.4	99.5		+5.8	15.1	-
	Replicate							43	-1.5	99.9				
GM1335	Kakortokite	448	+2.7	97.0	5.3*	-171*	0.21	41	-1.0	99.4	5.2	+3.7	11.8	+0.1
	Replicate 1	482	+3.4	97.8				39	+0.1	99.4				
	Replicate 2							38	-0.8	99.1				
GM1337	Kakortokite	655	(+4.6)	82.9	5.5*	-171*	0.25	37	-3.8	97.6	5.4	+6.1	19.5	+0.1
	Replicate 1	685	+2.2	98.6				35	-3.5	98.0				
	Replicate 2	722	+2.5	99.4										
XL61	Kakortokite	650	-0.1	99.7		-184		Absent	-	-	-			
	Replicate	604	+1.2	99.7										
XL63	Kakortokite	678	+3.8	97.8		-172		45	-0.3	99.8		+4.1	15.1	-
GM1843	Lujavrite	2104	+2.1	98.3	5.5*	-132*		35						
	Replicate	2346	+1.7	96.5				31	-1.7	98.3				
GM1294	Lujavrite	2865	+1.7	97.7		-219	0.33	30	-6.4	98.9		+8.4	82.0	-
	Replicate	2548	+2.0	99.1				29	-6.5	99.2				
GM1272	Lujavrite	1407	+1.2	97.3		-186	0.28	Absent	-	-	-			
ILM157	Lujavrite	2244	+0.4	99.3	5.4	-197	0.29	23	-7.9	94.9	5.1	+8.5	97.9	+0.3
	Replicate	2258	+0.7	99.0										
ILM145	Lujavrite	2670	+0.5	98.5		-211		35	-6.3	99.3		+6.4	76.3	-
	Replicate	-	-0.3	98.2										
<i>Late-stage</i>														
GM1390	Pegmatite	1373	+2.2	#	5.4*	-189*	0.31	22	+1.3	98.0	5.2*	+1.1	62.4	+0.2
	Replicate	-	+2.5	#										
ILM135	Pegmatite	923	+2.0	99.4	5.6	-122		65	+0.1	98.8	5.4	+2.3	14.4	+0.2
	Replicate							63	-0.7	99.5				
GM1657	Pegmatite	1754	+1.1	99.5		-167	0.26	Absent	-	-	-			
	Replicate	-	+1.1	99.3										
GM1257	Vein cutting IIIa rocks	Absent						84	-1.7	98.5	5.6*	-	-	-
ILM165	Vein cutting IIIb rocks	Absent						63	-1.4	99.2	5.2	-	-	-

(continued on next page)

Table 2b (continued)

Sample	Rock type	Amphibole						Clinopyroxene				$\Delta^7\text{Li}$ (amph-cpx) (‰)	$D_{\text{amph-cpx}}$	$\Delta^{18}\text{O}$ (amph-cpx) (‰)
		Li (ppm)	$\delta^7\text{Li}$ (‰)	Li yield (%)	$\delta^{18}\text{O}$ (‰)	$\delta D$ (‰)	$\text{Fe}^{3+}/\Sigma\text{Fe}$	Li (ppm)	$\delta^7\text{Li}$ (‰)	Li yield (%)	$\delta^{18}\text{O}$ (‰)			
ILM192	Vein cutting country rock granite	Absent						25	+8.6		3.7	–	–	–
GM1246	Vein cutting IIIa rocks	3137	+2.2	97.8	5.4	–172	0.32	Absent	–	–	–			
GG02	Vein cutting IIIb rocks	1463	+2.0	99.2	4.7**	–227		Absent	–	–	–			
ILM124	Vein cutting IIIa rocks	2089	+2.7	97.6	4.7	–179		42	–2.3	99.1	5.7**	+5.2	50.3	–1.0
		–	+3.3	99.4				41	–2.1	99.3				
ILM101	Aplite cutting IIIb rocks	1407	+5.4	96.1	5.2	–197	0.29	28	–1.4	99.6	4.8	+6.6	55.5	+0.4
		1370	+5.0	99.2				22	(–0.2)	93.9				
GM1212	Dyke (w.r.) cutting IIIa rocks	1904	+1.9	#	5.6*	–173*								
		1630	+2.9	#										

#=no monitoring of the Li yield, \*=data from Marks et al. (2004), \*\*=data from Graser & Markl (in revision), (w.r.)=whole-rock sample.  $\text{Fe}^{3+}/\Sigma\text{Fe}$  values are based on Mössbauer spectrometry.  $\delta^7\text{Li}$  values in parentheses were not used due to loss of Li during column separation (see Analytical methods section for details).

established ranges (e.g., Teng et al., 2006a,b) and JB-2 yielded  $+4.4\pm 0.6\text{‰}$  ( $2\sigma$ ,  $n=3$ , cf. published values ranging between +3.9 and +6.8, Magna et al., 2004, Jeffcoate et al., 2004, and references therein).

Since large Li isotope fractionation occurs during ion-exchange chromatography (Taylor and Urey, 1938), monitoring the Li yield from column chemistry by measuring before and after cuts is an important way to evaluate the quality of the Li isotope data. The Li yield during column separation was  $\geq 97\%$  in nearly all samples (Tables 2a,b and 3). Replicate analyses, described below, demonstrate that up to 5% Li loss does not affect the isotopic composition within analytical precision. For nearly all samples, two, and in some cases three, aliquots of dissolved mineral were processed through the ion-exchange columns as an additional test of the reproducibility of the method. In these cases, the average Li isotopic composition of the replicates is used as the “true” value. In the rare cases where a greater Li loss led to significantly different Li isotopic compositions, we processed a third aliquot of the sample. The average isotopic composition for these samples was then calculated by excluding the aliquot showing Li loss during column work.

Li concentrations were determined by comparing the voltage obtained for the sample with that of the two L-SVEC standards of known concentration, run on either side of a given sample, and then adjusting for sample weight. The precision and accuracy of this method is better than 10% (Teng et al., 2004a).

The oxygen isotope composition of the mineral separates and whole-rocks from the country rocks were determined by laser fluorination using a method adapted from Sharp (1990) and Rumble and Hoering (1994). Details of the method are described in Marks et al. (2003). Oxygen isotope compositions of some of the powdered whole-rock samples from the Ilímaussaq complex were determined by a conventional method modified after Clayton & Mayeda (1963) and Vennemann and Smith (1991) using  $\text{BrF}_5$  as reagent and converting the liberated oxygen to  $\text{CO}_2$ . The D/H ratios of the separates and whole-rock country rocks were determined according to a method adapted from Sharp et al. (2001). The hydrogen isotope compositions of the powdered whole-rock samples from the complex were determined according to the method of Vennemann and O’Neil (1993). Oxygen isotopic compositions were measured at the Institut für Geowissenschaften of the Universität Tübingen, Germany, using a Finnigan MAT 252 isotope ratio mass spectrometer and at the Institut de Minéralogie et Géochimie, Lausanne. Measurements of the hydrogen isotope compositions were also performed at the Institut de Minéralogie et Géochimie, Lausanne using high-temperature (1450 °C) reduction methods with He-carrier gas and a TC-EA from Thermo-Finnigan linked to a Delta Plus XL mass spectrometer. The results are given in the standard  $\delta$ -notation and are expressed relative to V-SMOW in permil (‰). Replicate oxygen isotope analyses of the standards (NBS-28 quartz and UWG-2 garnet; Valley et al., 1995) gave an

Table 3

Li concentration, Li, O and H isotope data and the Li yield from column chemistry of whole-rock samples from granitic basement rocks and basaltic as well as sedimentary rocks from the Eriksfjord formation along with their distance to the augite syenite unit (phase I)

Sample	Rock type	Distance to augite syenite unit	Li (ppm)	$\delta^7\text{Li}$ (‰)	Li yield (%)	$\delta^{18}\text{O}$ (‰)	$\delta D$ (‰)
EF 24	Basalt	Several km	9.6 <sup>§</sup>	+2.8 <sup>§</sup>	99.0 <sup>§</sup>	4.3 <sup>§</sup>	-102
EF 72	Basalt	Several km	7.6 <sup>§</sup>	+5.3 <sup>§</sup>	99.0 <sup>§</sup>	5.5 <sup>§</sup>	-92
EF 168	Basalt	Several km	43.3 <sup>§</sup>	-0.2 <sup>§</sup>	99.3 <sup>§</sup>	3.8 <sup>§</sup>	-73
EF 21	quartzite	Several km	10.3	+19.1	98.1	11.5 <sup>**</sup>	n.a.
EF 28	Arkose	Several km	73.3	+4.4	99.1	6.8 <sup>**</sup>	-101
ILM 194	quartzite	Xenolith within augite syenite	20.3	+6.3	99.1	10.3	n.a.
BT 3	Granite	Several km	4.6	+0.4	99.0	8.2 <sup>*</sup>	-109
BT 5	Granite	Several km	11.3	+4.7	98.8	7.2 <sup>*</sup>	-109
BT 6	Granite	Several km	12.8	+1.2	98.9	7.9 <sup>*</sup>	-96
JG 2	Granite	Several km	10.3	+6.3	99.5	7.8 <sup>**</sup>	-106
JG 5	Granite	~225 m	13.7	+4.2	97.5	5.0	-83
JG 6	Granite	~200 m	13.7	+3.9	98.2	5.3	-100
JG 7	Granite	~175 m	18.5	+4.7	97.9	5.8	-104
JG 8	Granite	~120 m	20.4	+18.4	95.7	8.5	-104
			21.0	+18.4			
JG 9	Granite	~90 m	20.3	+6.0	94.4	6.3	-104
JG 10	Granite	~45 m	341.8	+5.8	95.9	7.0	-123
JG 11	Granite	~5 m	18.1	-9.0	99.1	6.7	-110
JG 12	Granite	~2 m	28.1	-1.4	96.5	6.9	-109
JG 13	Granite	0.2 m	31.1	+1.0	98.3	7.1	-112

\* = data from Halama et al. (2004), \*\* = data from Halama et al. (2003),

§ = data from Halama et al. (in revision), n.a. = not analyzed.

average precision of  $\pm 0.2\text{‰}$  for  $\delta^{18}\text{O}$  values. The precision of the in-house kaolinite standard and NBS-30 biotite for hydrogen isotope analyses was better than  $\pm 3\text{‰}$ ; all values are normalized using a value of  $-125\text{‰}$  for this kaolinite standard and  $-65\text{‰}$  for NBS-30, both of which were analyzed during the same period as the amphiboles.

Whole-rock X-ray fluorescence (XRF) analyses were performed using a Bruker S4 Pioneer machine at the Institut für Geowissenschaften, Universität Tübingen. The samples were crushed and milled in an agate mill and the powder dried at  $100\text{ °C}$  before melting it for the fusion discs. Detection limits for trace elements varied

between 1 (Eu, Yb, U) and 10 ppm (Ba, Ce, Pb). For calibration, a set of 35 international rock standards was used (compiled in Govindaraju, 1989) and, based on this, the estimated uncertainty is generally  $<5\%$  for major elements and  $<10\%$  for trace elements.

Mössbauer spectrometry for the measurement of the  $\text{Fe}^{3+}/\Sigma\text{Fe}$  ratio of representative amphibole separates was performed at the Bayerisches Geoinstitut in Bayreuth/Germany. Mössbauer spectra were recorded at room temperature (293 K) in transmission mode using the procedure reported in Enders et al. (2000). Values of  $\text{Fe}^{3+}/\Sigma\text{Fe}$  were determined from the relative area ratios corrected for recoil-free fraction effects based on the Debye model (e.g., McCammon 2004) and the riebeckite data of Van Alboom and De Grave (1996). A total error of about  $\pm 2\%$  (absolute) was estimated based on counting statistics and uncertainties in the fitting model.

## 5. Results

### 5.1. O and H isotopic compositions

#### 5.1.1. Ilímaussaq minerals

New oxygen isotope data for pyroxene and amphibole from the augite syenite unit vary between  $+5.2$  and  $+5.8\text{‰}$ , and are similar to previously published data (Fig. 4, Table 2a; Marks et al., 2004). Four out of the five samples show negative  $\Delta^{\text{amph-cpx}}$  values between  $-0.2$  and  $-0.6\text{‰}$  consistent with oxygen isotope equilibrium (e.g., Zheng, 1993a,b). However, the relatively small  $\Delta^{\text{amph-cpx}}$  values compared to the precision of the data ( $\pm 0.2\text{‰}$ ) make it difficult to calculate a temperature of equilibration.  $\delta D$  values for amphiboles and biotite vary between  $-101$  and  $-78\text{‰}$  and between  $-86$  and  $-71\text{‰}$ , respectively. In the four amphibole- and biotite-bearing samples, the latter is consistently enriched in D, indicating hydrogen isotope disequilibrium (Suzuoki and Epstein, 1976). This is consistent with the petrographic evidence that biotite formed later than amphibole and implies that the  $\delta D$  value of later stage fluids was higher compared to earlier fluids.

In the other samples, most amphiboles and aegirines have a similar range in  $\delta^{18}\text{O}$  between  $+5.7$  and  $+4.7\text{‰}$  (Table 2b) and, in contrast to the augite syenite, positive  $\Delta^{\text{amph-cpx}}$  values for all but one sample indicate oxygen isotope disequilibrium (Table 2b, Zheng, 1993a,b). Exceptionally  $^{18}\text{O}$ -depleted aegirine occurs in the peralkaline granite ( $+3.7\text{‰}$ ) and in an aegirine-vein ( $+3.1\text{‰}$ ) intruding the basement granite.  $\delta D$  values of amphiboles from the other rock types have unusually low  $\delta D$  values of  $<-120\text{‰}$ .

### 5.1.2. Country rocks

Oxygen and hydrogen isotope data for country rocks are presented in Table 3. Basalts have relatively low and variable  $\delta^{18}\text{O}$  values (+3.8 to +5.3‰), possibly reflecting alteration of the samples (Halama et al., in revision). One arkose has a  $\delta^{18}\text{O}$  value of +6.8‰ and quartzites have the highest  $^{18}\text{O}$  enrichment with values of around +11‰. Granites sampled far away from the Ilímaussaq complex have a relatively small range in their  $\delta^{18}\text{O}$  and  $\delta D$  values ( $\delta^{18}\text{O}$ =+7.2 to +8.2‰,  $\delta D$ =−96 to −109‰), with values typical for I-type granitoids (e.g., Taylor, 1986).

Granites sampled near the complex generally have lower  $\delta^{18}\text{O}$  values, but they decrease with increasing distance from the augite syenite unit from  $\sim$ +7‰ near the contact, down to  $\sim$ +5‰ far removed from the contact. The exception is again sample JG 8, which has a high  $\delta^{18}\text{O}$  value of +8.5‰.  $\delta D$  values vary between −83 and −123‰.

### 5.2. Li concentrations

#### 5.2.1. Ilímaussaq minerals and whole-rocks

In amphibole [Li] are highly variable and generally increase with igneous differentiation (Tables 2a and 2b, Fig. 2a). The lowest [Li] (7–68 ppm) are found in Ca-amphiboles of the augite syenite (phase I), where two samples have relatively low concentrations (7 and 21 ppm, respectively) and the remaining three samples have similar [Li], between 54 and 68 ppm. Na-amphiboles of the peralkaline granite and the apgaites (phases II and III) have significantly higher [Li], increasing from about 400 ppm to >2600 ppm. Variable and even higher [Li] (>3100 ppm) is found in Na-amphibole from late-stage veins.

Compared to amphiboles, [Li] in clinopyroxene are low (15–84 ppm), with no systematic differences between the different intrusive units, hence degree of differentiation (Tables 2a and 2b; Fig. 2b). However, it is noteworthy that within the augite syenite, the lowest [Li] in clinopyroxene is found in the same two samples having low [Li] in amphiboles.

Biotite only occurs in appreciable amounts in four out of the five samples of augite syenite. Their [Li] vary between 95 and 212 ppm (Table 2a) and, as for amphiboles and clinopyroxenes, the outermost sample has the lowest [Li] (95 ppm) and the three other samples have similar [Li], between 190 and 227 ppm.

[Li] in augite syenite whole-rock samples reflect the same trends as the minerals, with low [Li] (7 ppm) in the outermost chilled sample and higher [Li] (about 25 ppm) in the inner parts of the unit.

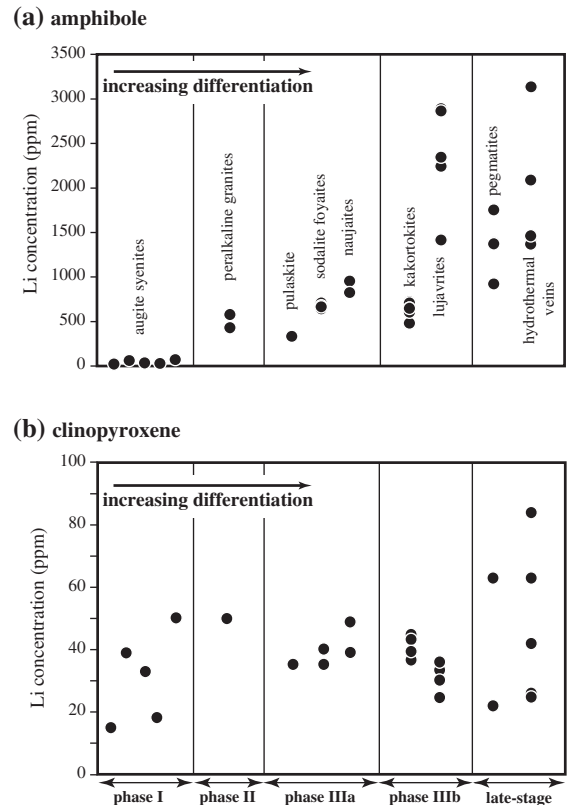


Fig. 2. Li concentrations in (a) amphibole and (b) clinopyroxene of the different intrusive phases of the Ilímaussaq intrusion, shown in order of increasing differentiation. Analytical uncertainty is smaller than the symbol size.

#### 5.2.2. Country rocks

[Li] for various country rocks are presented in Table 3. Basalts from the Eriksfjord formation have variable [Li] between 8 and 43 ppm, one arkose has 73 ppm Li and two quartzites contain 10 and 20 ppm Li. Granites sampled far away from the Ilímaussaq complex have [Li] of 5–13 ppm.

Granites sampled in the vicinity of the Ilímaussaq complex show interesting systematics: with increasing distance from the augite syenite, [Li] decrease by a factor of about two from 31 ppm down to 14 ppm. The latter value is similar to granites sampled far away from Ilímaussaq and is thus taken as representative of [Li] in the Julianehåb granite. Sample JG 10 has an exceptionally high [Li] of  $\sim$ 340 ppm and, compared to all other granite samples, has high alkalis, MnO, LOI, Rb, Zn, Nb and REE, but the lowest  $\text{SiO}_2$  and the lowest  $\delta D$  value of −123‰. Moreover, this sample contains sodic amphibole (with [Li] up to 3000 ppm (Kaliwoda, unpubl. data)), which likely accounts for the high [Li] found in the whole-rock; Tables 3 and 5.

Table 4  
Li-budget of the major Ilímaussaq rocks

	PHASE I	PHASE II	PHASE IIIa			PHASE IIIb	
	Augite syenite	Peralkaline granite	Pulaskite	Sodalite foyaite	Naujaite	Kakortokite	Lujavrite
<i>Mineral percentage</i>							
Feldspar	65–75	65–75	65–75	50–55	20–25	20–50	30–40
Quartz	–	15–20	–	–	–	–	–
Nepheline	0–3	–	5–10	4–8	4–8	15–20	10–25
Olivine	5–10	–	–	–	–	–	–
Magnetite	5–10	–	–	–	–	–	–
clinopyroxene	10–15	1–3	2–6	2–6	2–6	5–15	10–30
Amphibole	1–3	10–15	5–10	10–15	10–15	10–40	10–30
Biotite	1–3	–	–	–	–	–	–
Eudialyte	–	–	–	–	5–10	10–30	10–15
Sodalite	–	–	–	–	30–40	–	1–5
<i>Assumed Li concentration (ppm)</i>							
Feldspar	0.02	0.02	0.02	0.02	0.02	0.02	0.02
Quartz	–	1–20	–	–	–	–	–
Nepheline	5–30	–	5–30	5–30	5–30	5–30	5–30
Olivine	15–20	–	–	–	–	–	–
Magnetite	2	–	–	–	–	–	–
Clinopyroxene	<b>15–50</b>	<b>40–50</b>	<b>30–40</b>	<b>30–40</b>	<b>40–50</b>	<b>35–45</b>	<b>20–35</b>
Amphibole	<b>7–68</b>	<b>400–600</b>	<b>300–400</b>	<b>600–700</b>	<b>800–1000</b>	<b>400–700</b>	<b>2000–2800</b>
Biotite	<b>95–227</b>	–	–	–	–	–	–
Eudialyte	–	–	–	–	20–60	20–60	20–60
Sodalite	–	–	–	–	5–20	5–20	5–20
<i>Li in whole-rock (ppm)</i>	7–25	100–160	90–150	150–250	130–180	120–290	150–750
<i>% of total Li</i>							
Amphibole	5–20	>90	>75	>85	>85	>80	>85
Clinopyroxene	35–50	<3	<10	<3	<3	<10	<10
Biotite	25–50	–	–	–	–	–	–

Modal mineral percentages are after Ferguson (1964) and own observations, Li concentrations for whole-rocks are from Bailey et al., 2001 (except for the augite syenite) and Li concentrations for other minerals than clinopyroxene, amphibole and biotite are unpublished data from Kaliwoda. The data from the present study are indicated in bold; see also Tables 2a and 2b).

### 5.3. Li budget of the Ilímaussaq rocks

Based on whole-rock [Li], modal mineral abundances and [Li] in the major minerals (Bailey et al., 1993; Bailey and Gwodz, 1994; unpubl. data from M. Kaliwoda, Tübingen and data from the present study, see Tables 2a and 2b) we estimate the Li budget of the Ilímaussaq rocks (excluding pegmatites and hydrothermal veins) from mass balance (Table 4). A combination of changing phase proportions and [Li] cause the major host for Li to vary between the augite syenite and the other units. Augite and biotite (if present) are the important Li hosts in the augite syenite, containing about 35–50% and 25–50%, respectively, of the total Li, and Ca-amphibole is of minor importance (accounting for only 5–20%). For the other rock types, the picture is much simpler: Na-amphibole clearly dominates the Li budget in these rocks (containing  $\geq 75\%$  of the total Li) and aegirine incorporates at most 10%

(Table 4). Thus, in these rocks, the  $\delta^7\text{Li}$  values of amphiboles approximate that of the whole-rocks.

### 5.4. Li isotopic compositions

#### 5.4.1. Ilímaussaq minerals and whole-rocks

The  $\delta^7\text{Li}$  values of the analyzed minerals span a wide range, from +17 to  $-8\%$  (Tables 2a and 2b; Fig. 3). Augite syenites (phase I) have the greatest variability in  $\delta^7\text{Li}$ , with mineral isotopic compositions correlating with position within the intrusion. The  $\delta^7\text{Li}$  values are highest in the outermost sample ( $\sim +17\%$ ), and decrease systematically towards the inner part of this unit, with the lowest values occurring in the innermost sample ( $\sim +1\%$ ), which is adjacent to the agpaites (phase III). The whole-rock samples reveal a similar pattern, with low  $\delta^7\text{Li}$  values of about +2‰ for the two inner samples, increasing to a value of +14‰ in the outermost sample. In contrast, minerals from the two

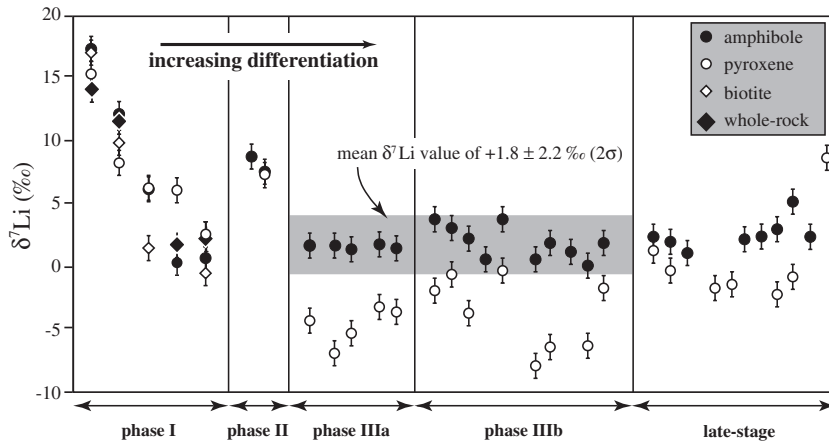


Fig. 3. Li isotope composition of mafic minerals (amphibole, clinopyroxene, biotite) from the different intrusive phases of the Ilímaussaq intrusion. Error bars represent  $2\sigma$  uncertainty of  $\pm 1\%$ .

samples of peralkaline granite (phase II) are homogeneous, with  $\delta^7\text{Li}$  varying within analytical uncertainty (+7.5 to +8.8‰). Within the agpaite suite,  $\delta^7\text{Li}$  of amphiboles are rather homogeneous, with an average value of  $+1.8 \pm 2.2\%$  ( $2\sigma$ ). In contrast, coexisting aegirines are consistently lighter than amphiboles and are highly heterogeneous, with  $\delta^7\text{Li}$  varying unsystematically from  $-7.9$  to  $+1.3\%$ . Amphiboles from late-stage pegmatites and veins have  $\delta^7\text{Li}$  values indistinguishable from amphiboles of phase IIIa and IIIb samples, despite the fact that the latter crystallized from melts, whereas amphiboles from hydrothermal veins are assumed to have precipitated from a late-stage fluid. Aegirine from the vein intruding the granite (sample ILM 192) has an exceptionally high  $\delta^7\text{Li}$  of  $+8.6\%$ , similar to aegirine from the peralkaline granite (see above).

#### 5.4.2. Country rocks

The  $\delta^7\text{Li}$  values of the country rocks span a wide range, from  $+19$  to  $-9\%$  (Table 3), with nearly the entire range seen in the granite traverse sampled adjacent to the contact of the augite syenite. Basalt  $\delta^7\text{Li}$  varies between  $+5.3$  and  $-0.2\%$ , correlating negatively with [Li] and partly reflecting low-temperature alteration (Halama et al., in revision). Two quartzites and the one arkose have variable  $\delta^7\text{Li}$  values between  $+4$  and  $+19\%$ . Granites sampled far away from the Ilímaussaq complex have  $\delta^7\text{Li}$  values between  $0$  and  $+6\%$ , overlapping with literature data for I-type granitoids ( $\delta^7\text{Li} = -2.5$  and  $+8\%$ ; Teng et al., 2004a,b; Bryant et al., 2004).

Granites in the vicinity of the complex show remarkable systematics; the  $\delta^7\text{Li}$  values of the three granites sampled closest to the augite syenite unit (JG

13–11) systematically decrease from  $+1$  to  $-9\%$  and all but one of the remaining granites have  $\delta^7\text{Li}$  values between  $+4$  and  $+6\%$ . Sample JG 8 has by far the highest  $\delta^7\text{Li}$  value of  $+18\%$  within this group; this sample also has exceptionally high  $\delta^{18}\text{O}$  of  $+8.5\%$ , but is petrographically indistinguishable from the other granite samples.

## 6. Discussion

### 6.1. Oxygen and hydrogen isotopic overprinting

The disequilibrium in oxygen isotopes between amphibole and clinopyroxene in all rocks except the augite syenites suggests that there has been subsolidus exchange between rocks and fluids. Since amphibole and pyroxene probably have similar closure temperatures for oxygen diffusion (700–800 °C; Farver and Giletti, 1985; Farver, 1989), the isotopically light composition of pyroxene must reflect crystallization from an isotopically distinct source at temperatures lower than 700 °C. This is consistent with the texturally later appearance of aegirine compared to amphibole and with the evidence for extensive hydrothermal activity in these rocks occurring at relatively low temperatures (Table 1). At such low temperatures (e.g.,  $<400$  °C), the  $^{18}\text{O}/^{16}\text{O}$  of a fluid phase will be lower than that of coexisting aegirine ( $1$ – $2\%$ ; Zheng, 1993a) and thus quite different from a typical magmatic fluid. Given the relatively low  $\delta^{18}\text{O}$  values of granites in the vicinity of the Ilímaussaq intrusion (Table 3), it appears that hydrothermal fluid circulation induced by the intrusion of the Ilímaussaq melts caused mixing between magmatic fluid with externally derived low  $\delta^{18}\text{O}$  fluids, from which aegirines crystallized at relatively low

temperatures. The exceptionally low  $\delta^{18}\text{O}$  values for aegirine occurring in the peralkaline granite (+3.7‰) and in an aegirine-vein (+3.1‰) intruding the basement granite underline the importance of externally derived aqueous fluids.

The unusually light  $\delta D$  in amphiboles from phase II, III and late-stage samples also reflect open-system behavior. They likely result from interaction and re-equilibration with D-depleted fluids originating from late-stage magmatic oxidation of internally generated  $\text{CH}_4$  and/or  $\text{H}_2$  (see Marks et al., 2004 for a detailed discussion).

### 6.2. Lithium substitution and partitioning between amphibole and clinopyroxene

In Na-amphiboles, Li occupies the M3-site, where it mainly substitutes for  $\text{Fe}^{2+}$  via the coupled substitution  $\text{Li}^+ + \text{Fe}^{3+} = 2 \text{Fe}^{2+}$  (e.g., Hawthorne et al., 1994; Marks et al., 2003), hence Li may play a role in charge balance during iron oxidation. Fig. 5 shows that [Li] in Na-amphiboles correlate positively with their  $\text{Fe}^{3+}/\text{Fe}^{2+}$  ratio, and if amphibole  $\text{Fe}^{3+}/\text{Fe}^{2+}$  reflects the magmatic redox state, as suggested by Della Ventura et al. (2005), [Li] thus also reflect oxygen fugacity. Such an increase in oxygen fugacity from early to late agpaite rocks and even more oxidized conditions during the hydrothermal stage is in accordance with previous petrological studies on the peralkaline igneous rocks of South Greenland (Markl et al., 2001; Marks et al., 2003, 2004).

In clinopyroxene, Li enters the M2-site, mainly substituting for Na (Brenan et al., 1998a; Thompson and Downs, 2003). Redhammer et al. (2001) demonstrated a complete solid solution between aegirine and Li-aegirine, hence Li and Na compete for the same crystallographic site. The high Na concentrations of the Ilimaussaq clinopyroxenes (typically around 12 wt.%  $\text{Na}_2\text{O}$ ; Markl et al., 2001) coupled with low [Li] (<85 ppm; Tables 2a and 2b) may therefore be a consequence of charge balance during iron oxidation occurring primarily through coupled substitution of Na and  $\text{Fe}^{3+}$ , which is in accordance with the strong correlation observed between those two cations (Markl et al., 2001).

In the augite syenites, where textures and oxygen isotope compositions indicate equilibration, amphibole–clinopyroxene Li abundance ratios ( $D_{\text{amph-cpx}}$ ) vary between 0.5 and 1.7. The lowest values (0.5 and 1.2) occur in the two samples with exceptional low [Li] and are possibly overprinted by secondary processes (Tables 2a and 2b; see below). The three remaining samples have  $D_{\text{amph-cpx}}$  values between 1.4 and 1.7, and we believe that

this range reflects equilibrium partitioning of Li between these two phases. For all other rock types, oxygen isotope compositions indicate isotopic disequilibrium between amphibole and pyroxene, consistent with the late formation of aegirine compared to amphibole, and the  $D_{\text{amph-cpx}}$  values are significantly higher and vary about one order of magnitude (Tables 2a and 2b). This large increase is mainly due to relatively constant Li concentration in clinopyroxenes, and increasing [Li] in amphibole with magmatic fractionation.

Changing major element compositions of amphiboles (Ca-rich in phase I rocks, Na-dominated in the other rock types) may have exerted an influence on the incorporation of Li. Apparently, Li behaves more compatibly in Na-amphibole, as reflected in the extreme [Li] observed in these minerals (up to 3000 ppm), and may become an essential constituent of the amphibole. In this case, the Li-rich Na-amphiboles in the agpaite Ilimaussaq rocks may act as a major sink for Li in peralkaline systems, thus prohibiting equilibrium partitioning of Li between amphibole and other mineral phases according to Henry's law.

The extreme Li enrichment in the agpaite amphiboles may also be due to increasing oxygen fugacity and the role of Li in charge balance, as indicated by the positive correlation between Li and  $\text{Fe}^{3+}/\Sigma\text{Fe}$  in these amphiboles (Fig. 5). Such a correlation is not observed in clinopyroxenes, where higher  $\text{Fe}^{3+}$  contents are charge balanced by the incorporation of Na into the M2-site (Markl et al., 2001), which also accommodates Li (thus Li and Na compete for the same site in clinopyroxene). In contrast, incorporation of Na in the amphibole structure is limited, since  $\text{Na}^+$  only fits into the M4- and A-sites. Thus,  $\text{Na}^+$  cannot compensate for  $\text{Fe}^{3+}/\Sigma\text{Fe}$  ratios higher than 0.20, which is the proportion of ferric iron found in Li-free arfvedsonite. Higher  $\text{Fe}^{3+}/\Sigma\text{Fe}$  ratios may require Li for charge balance. In this case, Li does not compete with Na for the M4- and A-sites, but instead enters the M3-site (e.g., Hawthorne et al., 1994) and thus could play the main role in charge balancing the higher  $\text{Fe}^{3+}$  contents in amphibole. As a result, the increase in oxygen fugacity from early to late agpaite rocks and the associated increase of the  $\text{Fe}^{3+}/\Sigma\text{Fe}$  ratio in the melt causes incorporation of Li into the amphibole structure to accomplish charge balance and is an important factor influencing the distribution of Li between amphibole and pyroxene.

### 6.3. Li isotope systematics

Homogeneous oxygen and neodymium isotopic compositions of mafic minerals were previously interpreted

to reflect mantle derivation of the parental magma of the Ilímaussaq complex, which evolved by crystal fractionation in a closed system (Marks et al., 2004). Amphiboles dominate the Li budget of the inner part of the intrusion (phase III and late-stage samples) and show little variation in their Li isotopic compositions. Minerals from the peralkaline granite at the roof of the complex (phase II) are also homogeneous, but have distinctly higher  $\delta^7\text{Li}$  values than the inner intrusion. In contrast, samples from the outermost parts of the complex (phase I, augite syenite) show large and spatially systematic Li isotope variations, which, when considered along with the Li isotopic systematics of the adjacent granite country rocks, suggests kinetically induced isotope fractionation took place during final cooling of these rocks.

Based upon experimental isotope partitioning data (Wunder et al., 2006, 2007) and first-principle calculations, which show that heavier isotopes are more strongly bonded in higher coordination sites (Schauble, 2004), the expected  $\delta^7\text{Li}$  of the phases at equilibrium are as follows:  $\delta^7\text{Li}^{[4]}_{(\text{fluid})} > \delta^7\text{Li}^{[5+1]}_{(\text{amphibole})} > \delta^7\text{Li}^{[6]}_{(\text{mica})} > \delta^7\text{Li}^{[6]}_{(\text{cpx})}$  (where the superscripted numbers in square brackets represent the coordination number of the site for Li substitution). Below, we discuss the Li isotopic systematics of each of the intrusive phases and the Li isotopic fractionations between coexisting minerals, which vary between the different intrusive phases.

### 6.3.1. Homogeneous Li isotopic composition in the inner part of the complex

The homogeneous Li isotope composition of amphiboles from phase III rocks ( $+1.8 \pm 2.2\%$ ,  $2\sigma$ ) points to a homogeneous melt reservoir. This  $\delta^7\text{Li}$  value is on the lower end of the range for fresh MORB ( $\delta^7\text{Li} = +1.5$  to  $+5.2\%$ ; Moriguti and Nakamura, 1998; Chan et al., 2002; Elliott et al., 2006; Tomascak et al., in revision), OIB and arc lavas ( $\delta^7\text{Li} = +1$  to  $+11\%$ ; e.g., Moriguti and Nakamura, 1998; Tomascak et al., 1999a,b, 2000, 2002; Bouman et al., 2004; Chan and Frey, 2003; Pistiner and Henderson, 2003; Magna et al., 2006) and is similar to syenites from Oldoinyo Lengai ( $-0.6$  to  $+4.4\%$ ; Halama et al., 2007) and to a single syenite from Mexico ( $+2.1\%$ ; Romer et al., 2005). The Nd isotope data suggest derivation of the Ilímaussaq parental magma from an OIB-like mantle source (Marks et al., 2004), and the Li isotopic data are consistent with this interpretation. The lack of any systematic change in Li isotopic composition of amphiboles from early to late rocks (Fig. 3) is consistent with previous studies (Teng et al., 2004b, 2006b; Bryant et al., 2004; Halama et al., 2007) that show that magmatic differentiation on its own does not produce significant Li isotopic fractionation.

Interestingly, even amphiboles from pegmatites and late-stage hydrothermal veins have Li isotopic compositions that are indistinguishable from amphiboles from phase III samples. This contrasts with an observed fractionation of  $+4\%$  between fluids and minerals of the Tin mountain pegmatite (Teng et al., 2006b). Various experimental studies (e.g., Sood and Edgar, 1970; Edgar and Parker, 1974; Kogarko and Romanchev, 1977) have shown that water pressure and oxygen fugacity are critical factors influencing the formation and chemical evolution of peralkaline to agpaite melts. The low initial water contents and/or low oxygen fugacities typically found in such rocks prevent early exsolution of large amounts of an aqueous fluid (Kogarko, 1977; Khomyakov, 1995). Alkalis and volatiles are therefore retained in the melt until the final stages of differentiation, in which a hydrothermal fluid may separate from a low-temperature melt (Sørensen, 1997). At Ilímaussaq, at least some of the late-stage amphiboles are believed to have crystallized from late-magmatic fluids or supercritical fluid–melt mixtures (Markl & Baumgartner, 2002). If some amphiboles crystallized from exsolved hydrothermal fluids, one would expect to see an effect on their Li isotopic composition compared to earlier amphiboles, since aqueous fluids are known to preferentially concentrate the heavier isotope  $^7\text{Li}$  relative to coexisting minerals (e.g., Chan et al., 1992; Zhang et al., 1998; Teng et al., 2006b; Wunder et al., 2006, 2007). However, if this phase separation occurs under supercritical conditions, no Li isotopic fractionation is expected (Foustoukos et al., 2004) and this may explain the similarity in  $\delta^7\text{Li}$  of late-stage minerals inferred to have crystallized from such fluids.

Amphiboles in all of these samples are consistently heavier than pyroxenes.  $\Delta^7\text{Li}_{\text{amph-cpx}}$  is highly variable ( $+1$  to  $+8\%$ ; Table 2b; Fig. 3) and does not show any systematic behavior (e.g.,  $\Delta^{\text{amph-cpx}}$  does not correlate with rock type, texture, nor estimated equilibration temperature). Thus, we conclude that amphibole–pyroxene pairs are generally not in Li isotopic equilibrium, in accordance with the observed oxygen isotopic disequilibrium. Experimental studies document that, compared to other elements, Li diffusion in melts, minerals and fluids is very rapid (Richter et al., 2003; Giletti and Shanahan, 1997; Coogan et al., 2005) and samples in which diffusion has been incomplete can record profiles with large isotopic fractionations (e.g., Richter et al., 1999; Lundstrom et al., 2005; Teng et al., 2006a). Indeed, several recent studies (e.g., Beck et al., 2006; Barrat et al., 2005; Jeffcoate et al., 2007; Parkinson et al., 2007) document large variations of  $\delta^7\text{Li}$  (up to several tens of per mil) within single

clinopyroxene crystals (several 100  $\mu\text{m}$  large). Li isotopic core–rim profiles of such crystals generally have central minimum values. These large  $\delta^7\text{Li}$  variations are suggested to be due to diffusional uptake of lithium, with  $^6\text{Li}$  moving into the crystal faster than  $^7\text{Li}$  (giving rise to low  $\delta^7\text{Li}$ ). Modeling shows that, with time, the low  $\delta^7\text{Li}$  zones broaden and migrate towards the centre of the crystals (Parkinson et al., 2007). Thus, the observed Li isotopic fractionation between amphibole and clinopyroxene in our samples may also reflect diffusion of Li into the clinopyroxene from a Li-rich phase (melt, the amphibole and/or a fluid). The fact that amphiboles are isotopically more homogeneous than clinopyroxenes probably reflects mass-balance (amphiboles have much higher Li contents than pyroxenes and thus are less affected by kinetic fractionation) or significantly faster diffusivity of Li in amphibole compared to clinopyroxene, as has been inferred for clinopyroxene compared to olivine (Jeffcoate et al., 2007; Rudnick and Ionov, 2007; Parkinson et al., 2007).

### 6.3.2. Homogeneous but heavy Li isotopic composition at the roof of the complex

Based on oxygen and Nd isotopic data, this unit appears to have experienced significant assimilation (about 13%) of evolved, deep crustal rocks (Stevenson et al., 1997; Marks et al., 2004). The two peralkaline granites have a homogeneous Li isotopic composition of about +8‰ with a whole-rock Li-concentration of 100–150 ppm (Bailey et al., 2001; Kaliwoda, unpubl. data). The lower crust is assumed to have a mean Li concentration of about 13 ppm (Rudnick and Gao, 2003), although Li concentrations of deep crustal samples vary from 1 to 60 ppm (Mengel, 1990; Teng et al., 2004b) with Li concentrations generally higher in more evolved samples (Teng et al., 2004b). Nevertheless, it is difficult to explain the relatively heavy Li isotope composition of the peralkaline granite via crustal contamination. Even assuming that the evolved lower crust has an extreme Li content of 60 ppm and that the melt giving rise to the peralkaline granites originally had a Li content similar to that of the augite syenite (20 ppm) requires the deep crustal assimilate to have a  $\delta^7\text{Li}$  of  $>+20\text{‰}$  assuming 13% assimilation, as suggested by the Nd and O isotope data. This  $\delta^7\text{Li}$  value is higher than any rock ever measured (the highest rocks are sea-water altered MORB, with  $\delta^7\text{Li}$  values up to +14‰ (Chan et al., 1992) and a single lower crustal xenolith at +16‰ (Teng et al., submitted for publication). In contrast, limited Li isotopic data indicate that the lower crust is highly heterogeneous (e.g.,  $\delta^7\text{Li}$  –16 to +16‰), with an average  $\delta^7\text{Li}$  value near 0‰. Thus it

is unlikely that assimilation of deep crustal rocks can explain the Li isotopic composition of the peralkaline granite.

Alternatively, extensive crystal fractionation with  $D > 1$  (e.g., Na-amphibole; see above) could increase  $\delta^7\text{Li}$  by several permil (see Teng et al., 2006b). However, this is also not an adequate explanation for the Ilmaussaq peralkaline granites, since they are less fractionated than the aegaitic rocks.

No Li isotopic fractionation is seen between amphibole and pyroxene in the single granite sample for which both minerals were analyzed (Table 2b; Fig. 3), despite the strong oxygen isotopic disequilibrium (Table 2b; Fig. 4). In addition, aegirine from this sample ( $\delta^7\text{Li} = +7.5\text{‰}$ ) is exceptionally enriched in  $^7\text{Li}$  compared to all other aegirines, but remarkably similar to aegirine from a hydrothermal vein intruding the country rock granite (ILM192,  $\delta^7\text{Li} = +8.6\text{‰}$ ) and both aegirines have similar low  $\delta^{18}\text{O}$  values of +3.7 and +3.1‰, respectively. Assuming crystallization temperatures between 300° and 400 °C for these aegirines, and applying equilibrium  $\Delta^7\text{Li}^{\text{cpx-fluid}}$  (Wunder et al., 2006) and  $\Delta^{18}\text{O}^{\text{cpx-fluid}}$  values (Zheng, 1993a), the coexisting fluid would have a  $\delta^7\text{Li}$  value of around +13‰ and a  $\delta^{18}\text{O}$  value of around +2‰. Both values are consistent with the assumption that the aegirines crystallized in equilibrium with externally derived aqueous fluids. Amphiboles from the peralkaline granite have a similar  $\delta^7\text{Li}$  value but a higher  $\delta^{18}\text{O}$  value. Thus, the only viable explanation is that both minerals re-equilibrated with a heavy Li source at low temperatures, but, because of slower diffusivity, oxygen in amphibole did not re-equilibrate (Farver, 1989; Farver and Giletti, 1985).

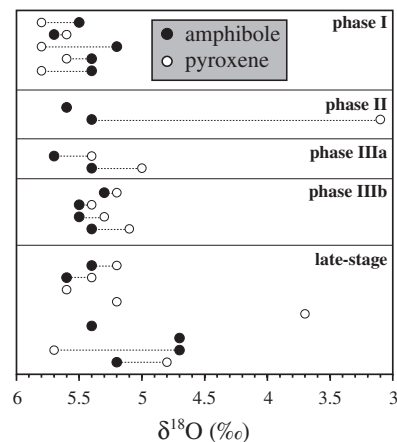


Fig. 4. Oxygen isotope data for amphibole and pyroxene separates from the Ilmaussaq complex.

### 6.3.3. Systematic changes in $\delta^7\text{Li}$ at the margin of the complex and in adjacent country rocks

The systematic and large change in  $\delta^7\text{Li}$  values from about +2‰ in the inner part of the marginal augite syenite unit (phase I) towards values of around +14‰ at its margin is striking. The Li isotopic systematics of the country rock granites adjacent to this unit yield additional insights into the processes that produced the fractionation. Important questions in this context are: i) What is the  $\delta^7\text{Li}$  of the parental melt of the augite syenite and ii) what processes produced the observed spatial systematics of the  $\delta^7\text{Li}$  values in the augite syenite and the adjacent country rock granites?

It is unlikely that the  $\delta^7\text{Li}$  of all five augite syenite samples reflect primary magmatic values since i) Li isotope fractionation during basalt (Tomascak et al., 1999a), granite (Bryant et al., 2004; Teng et al., 2004a) and alkaline magma (Halama et al., 2007) differentiation is not resolvable. The only documented Li isotope fractionation related to igneous processes to date is found in low temperature, late-stage pegmatites formed under hydrous conditions (Teng et al., 2006b), conditions significantly different from those prevalent during crystallization of the augite syenite ( $T > 600$  °C and  $a_{\text{H}_2\text{O}} = 0.2$ ; Marks and Markl, 2001; Markl et al., 2001). ii) All  $\delta^7\text{Li}$  values in primary, mantle-derived igneous rocks (MORB, OIB, carbonatites) are significantly lower than that of the most primitive augite syenite sample ( $\delta^7\text{Li} = +14$ ‰ for the chilled margin sample), averaging about +4‰ e.g., Moriguti and Nakamura, 1998; Tomascak et al., 2000, 2002; in revision; Chan et al., 2002; Bouman et al., 2004; Ryan and Kyle, 2004; Chan and Frey, 2003; Pistiner and Henderson, 2003; Elliott et al., 2006; Halama et al., 2007). Thus, other processes must have produced the systematic changes in Li isotopic compositions of the augite syenite minerals. These might include assimilation of country rocks, interaction with a fluid phase and/or Li diffusion, and we address each of these processes, in turn.

Country rock assimilation is unlikely to explain the systematic changes in  $\delta^7\text{Li}$  in the augite syenite for the following reasons: First, all samples are nepheline-bearing, which is inconsistent with assimilation of quartz-rich country rocks (granite, quartzites or sandstones). Second, the very heavy Li isotopic composition of the outermost sample ( $\delta^7\text{Li} = +14$ ‰) would require an even higher  $\delta^7\text{Li}$  value for the assimilant. The Li isotopic compositions of country rocks are highly variable (−9 to +19‰; Table 3), but only a quartzite and a single granite have such high  $\delta^7\text{Li}$  values, which are not representative of the exposed rocks. Finally, although xenoliths of quartzite several tens of meters

wide occur within the augite syenite, the amount of assimilation required (>80% bulk assimilation) to explain the high  $\delta^7\text{Li}$  value is neither consistent with the nepheline-bearing assemblages (Marks and Markl, 2001) nor with the oxygen isotope data of the sandstones, which are significantly heavier than the syenites (+10‰, Halama et al., 2003). Moreover, the high melting temperature of quartz (Tuttle and Bowen, 1958) precludes this possibility. Thus, contamination with country rocks is not a viable explanation for the heavy Li isotopic composition of the marginal augite syenites.

Instead, the systematic spatial changes in  $\delta^7\text{Li}$  values in both the augite syenite and surrounding granites (Fig. 6) is reminiscent of kinetic isotope fractionation produced by diffusion (Richter et al., 2003), which produces low  $\delta^7\text{Li}$  in the rock into which Li is diffusing (country granites) and high  $\delta^7\text{Li}$  in the rock that loses Li (augite syenite). Several recent studies have shown that Li diffusion produces large isotopic fractionation in rocks that are infiltrated by a Li-bearing fluid, and that, with time, these low  $\delta^7\text{Li}$  zones broaden and migrate away from the Li source (e.g., Teng et al., 2006b; Parkinson et al., 2007). Evidence for the infiltration of alkaline fluids transporting Li into the country rock granites is the increase in [Li] in granites sampled close to the augite syenite margin (Tables 3 and 5; Fig. 6) and the presence of sodic pyroxene and/or sodic amphibole in these samples. Sodic pyroxene has around 60 ppm Li (Kaliwoda, unpubl. data). Boron isotopes on the same samples also document fluid infiltration (Kaliwoda et al., 2007). Using a  $D_{\text{cpx-fluid}}$  value of 0.2 (Brenan et al., 1998b), we calculated that the fluid had ~300 ppm [Li]. We modeled the effects of Li diffusion from the syenite into the adjacent granites via fluid

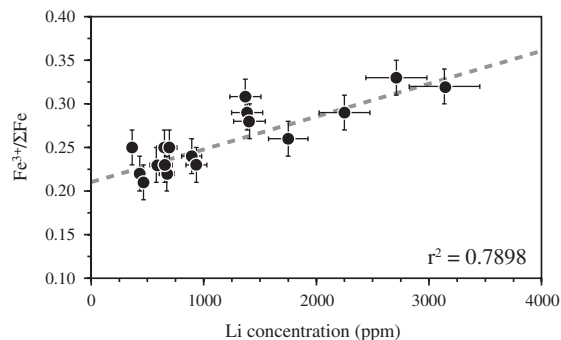


Fig. 5. Li concentration (ppm) versus  $\text{Fe}^{3+}/\Sigma\text{Fe}$  ratio (determined by Mössbauer spectrometry) for representative alkali amphiboles from the apgaitic Ilímaussaq rocks. For the  $\text{Fe}^{3+}/\Sigma\text{Fe}$  ratio an error of  $\pm 2\%$  (absolute) was estimated, and for the Li concentrations a relative error of 10% is assumed, based on replicate Li determinations.

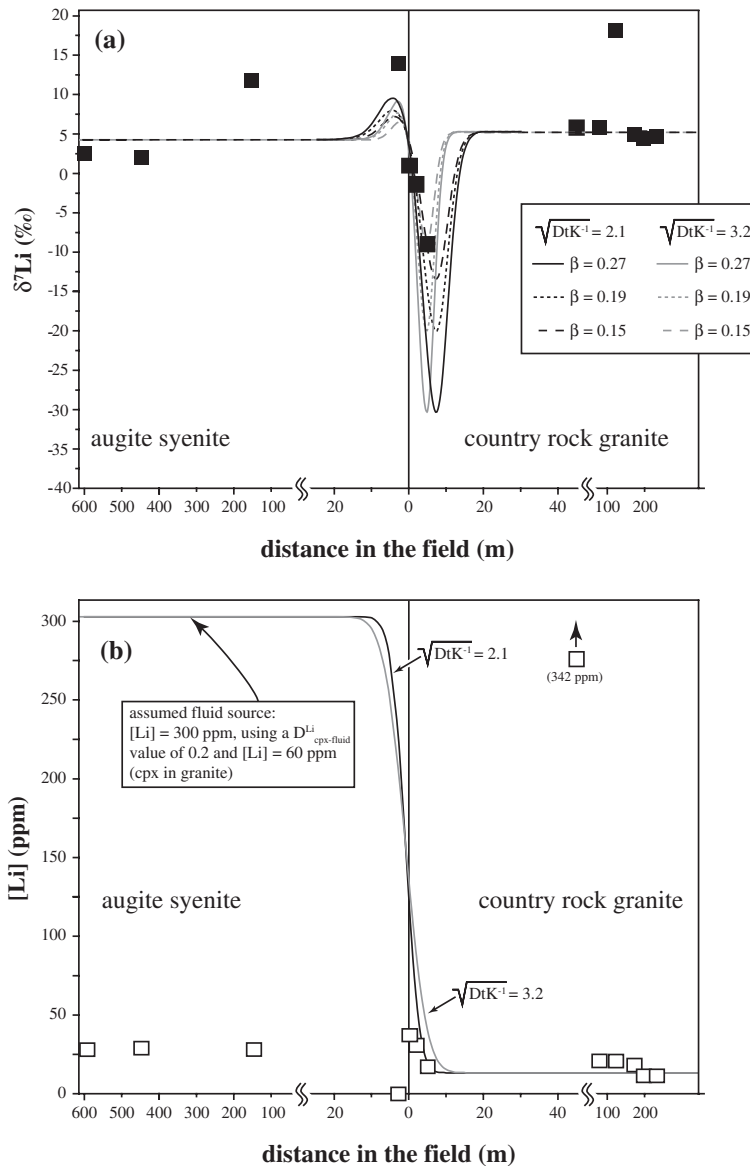


Fig. 6. Modeled curves for diffusion-induced lithium isotope fractionation across the contact between the marginal augite syenite unit (phase I) and adjacent country rock granites in comparison with measured Li isotopic compositions (a) and measured [Li] (b). For the modeling, we used initial  $\delta^7\text{Li}$  values of +4‰ for the fluid phase (estimated using the experiments of Wunder et al., 2007, assuming the fluid to be in isotopic equilibrium with the innermost augite syenite sample) and +5‰ for the country rock granites (average of far-field granite samples JG 2, 5, 6, and 7) and accordingly, the initial [Li] were chosen as 300 ppm (using a  $D_{\text{cpx-fluid}}$  value of around 0.2 (Brenan et al., 1998b)) and 14 ppm (average of far-field granite samples JG 2, 5, 6, and 7), respectively. See text for further details.

infiltration using a similar approach as Cartwright & Valley (1991). The change of Li concentration ( $C$ ) at distance ( $x$ ) with time ( $t$ ) is given by the following one-dimensional diffusion equation

$$C(x, t) = C^0 - \frac{\Delta C}{2} \operatorname{erfc}\left(\frac{x}{2\sqrt{DtK^{-1}}}\right)$$

(Crank, 1975), where  $\operatorname{erfc}$  is the complementary error function,  $C^0$  is the [Li] of the fluid phase,  $\Delta C$  is the initial concentration difference between the fluid phase and the country rock granite,  $D$  is the effective diffusivity and  $K$  the effective partition coefficient of Li between rock and assumed fluid. The diffusion curves for  $^6\text{Li}$  and  $^7\text{Li}$  were modeled separately and the

Table 5

Whole-rock analysis of samples from the augite syenite unit (phase I) of the Ilimaussaq complex and adjacent granitic rocks

	GM1857	GM1333	GM1330	GM1858	JG-13	JG-12	JG-11	JG-10	JG-9	JG-8	JG-7	JG-6	JG-5
sample	–600	–450	–150	–2	0.2	2	5	45	90	120	175	200	225
<i>(wt.%)</i>													
SiO <sub>2</sub>	55.68	55.294	53.62	53.83	66.95	68.14	68.87	64.60	70.39	72.21	70.74	71.52	70.68
TiO <sub>2</sub>	1.36	1.57	1.93	1.8	0.43	0.35	0.42	0.44	0.37	0.22	0.34	0.32	0.43
Al <sub>2</sub> O <sub>3</sub>	16.42	15.975	15.24	15.79	15.07	15.88	15.54	16.06	14.64	14.48	14.71	14.45	15.01
Fe <sub>2</sub> O <sub>3</sub>	9.81	10.236	11.80	11.6	0.55	0.81	1.40	1.46	0.93	0.52	1.09	0.90	1.60
FeO	n.d.	n.d.	n.d.	n.d.	2.60	1.66	1.35	0.50	1.19	0.96	0.95	0.99	0.76
MnO	0.22	0.23	0.26	0.24	0.07	0.05	0.04	0.15	0.04	0.03	0.04	0.04	0.03
MgO	0.94	1.31	1.47	2.24	1.34	0.96	0.73	0.68	0.81	0.46	0.81	0.82	1.55
CaO	4.07	4.09	4.50	4.88	2.20	2.27	1.67	1.25	1.27	1.43	1.07	0.81	0.35
Na <sub>2</sub> O	5.82	4.99	5.07	4.84	5.11	4.82	4.37	6.72	4.03	4.07	4.15	4.18	8.24
K <sub>2</sub> O	4.91	5.37	4.86	4.3	4.33	4.09	5.01	5.96	5.37	4.66	5.28	5.33	0.31
P <sub>2</sub> O <sub>5</sub>	0.44	0.52	0.71	0.55	0.19	0.18	0.14	0.12	0.13	0.07	0.13	0.12	0.12
LOI	0.24	0.06	0.15	0.02	0.10	0.26	0.21	1.27	0.32	0.27	0.23	0.25	0.59
Total	99.91	99.64	99.59	100.09	98.94	99.48	99.75	99.20	99.49	99.39	99.53	99.74	99.66
<i>(ppm)</i>													
Li	24.8	25.5	23.1	7.1	31.1	28.1	18.1	341.8	20.3	20.4	18.5	13.7	13.7
Ba	1932	2302	1933	3736	1043	793	876	145	788	938	847	750	69
Co	6	6.7	8.3	10.7	5.2	6.2	2	–	1.3	–	1	0.8	2.7
Cr	8.3	6.2	15.6	4.4	–	–	–	–	–	–	0	0	0
Ni	77	71	79	66	32	26	43	–	36	22	34	38	56
Rb	100	98	89	68	141	165	166	324	211	194	204	207	14
Sr	260	248	232	477	463	449	376	161	263	326	229	219	45
V	16	21	24	29	35	33	44	24	25	18	27	29	16
Y	72	62	75	48	25	19	17	23	21	5	16	18	17
Zn	166	150	186	143	65	58	47	505	36	20	35	26	38
Zr	500	386	443	287	281	209	262	178	233	142	196	204	323
Ce	146	119	139	77	148	120	135	219	133	66	93	102	184
Eu	0.8	0.8	0.8	1.2	1.6	1.4	1.5	1.3	1.1	0.9	0.9	1	1.1
La	36	15	34	21	76	68	87	157	69	40	43	61	97
Nb	103	73	88	49	–	17.1	–	298	17.7	–	–	14.9	23.7
Nd	80	65	86.3	42	52	42.2	52	74.6	45.7	23.4	31.2	33.7	64.8
Sm	260	260	260	260	9	6.8	10.4	15.4	9.2	5.2	6.8	8.8	11.8
Yb	5.8	5.1	6.1	3.8	1.9	1.6	1.3	2.4	1.8	0.6	1.4	1.6	1.4

–=below detection limit; n.d.=not determined.

resulting  $\delta^7\text{Li}$  value was calculated by combining the concentration curves for the two isotopes. The ratio of effective diffusion coefficients for  $^6\text{Li}$  and  $^7\text{Li}$  is related to their mass according to the equation  $D_6/D_7=(m_7/m_6)^\beta$  (Richter et al., 1999). Experimental studies show that  $\beta$  in melts or fluids is 0.215 or smaller (Richter et al., 2003; Fritz 1992). Teng et al. (2006b) inferred a  $\beta$  value of 0.15 for fluid-assisted Li diffusion into amphibolite country rocks from a Li-pegmatite, based on the shape of the diffusion profile, and Parkinson et al. (2007) inferred  $\beta$  values between 0.19 and 0.27; we thus allow  $\beta$  to vary within these boundaries. Initial [Li] and  $\delta^7\text{Li}$  values for the intrusion and the country rocks are taken from the innermost augite syenite and granites sampled far away from the intrusion, respectively (Tables 2 and 3). The position of the isotopic minimum

within the granite relative to the contact between the two rock types is determined by the parameters  $K$ ,  $D$  and  $t$ . The longer the time of diffusion ( $t$ ) and the larger the effective diffusivity ( $D$ ), and the smaller the effective partition coefficient ( $K$ ), the broader the isotopic minimum, the further it moves from the contact into the adjacent granites, and the flatter is the Li concentration profile at the border between them. None of these three parameters is actually known, but semi-quantitative constraints on them include the following:

- Although Li diffusivity in pure water is determined to be on the order of  $1 \times 10^{-5} \text{ cm}^2/\text{s}$  at 25 °C (Li and Gregory (1974); increasing with increasing temperature), it is not known how this relates to supercritical

fluids. Moreover, the porosity and tortuosity in the granites are not known. However it is likely that the effective diffusivity ( $D$ ) is significantly smaller than Li diffusivity in pure water.

- The effective partition coefficient ( $K$ ) is likely to be larger than the partition coefficient between rock and fluid (see discussion in Cartwright and Valley, 1991), and is estimated to vary between about 1 and 3.
- The maximum time of diffusion ( $t$ ) is equal to the age of the Ilímaussaq rocks (1.16 Ga, Krumrei et al., 2006).
- Using these constraints, we fitted the term  $\sqrt{DtK^{-1}}$  to our data points, resulting in values between 2.1 and 3.2 (both lower or higher values did not yield a reasonable fit). These values are the same order of magnitude as the results of Teng et al. (2006a) and using the age of the Ilímaussaq rocks to provide a minimum estimate of the effective diffusivity of Li within the granite, a value of  $\sim 1 \times 10^{-12}$  cm<sup>2</sup>/s is obtained, again very similar to the estimates of Teng et al. (2006a) for minimum  $D$  values for amphibolite.

This approach reproduces the observed  $\delta^7\text{Li}$  minimum within the granites (Fig. 6), but not the  $\delta^7\text{Li}$  maximum of the outermost augite syenite. The most critical factor determining the amplitude of Li isotope fractionation is the empirical factor  $\beta$ . The assumed concentration difference ( $\Delta C$ ) between the two units and their estimated initial  $\delta^7\text{Li}$  values are of only minor importance. The calculated curves still fit the data well even if the  $\delta^7\text{Li}$  value for the fluid phase is allowed to vary between +3 and +8, or its initial [Li] is assumed to be as low as 150 ppm. The larger  $\beta$  is chosen to be, the larger the possible amount of fractionation (and thus the amplitude of the isotopic minimum and maximum, respectively). If extremely large values for  $\beta$  are assumed ( $\geq 0.5$ ), fractionation of  $\sim 14\%$ , as observed in the augite syenite unit, can be modeled. However, such high  $\beta$  values are not realistic (see Richter et al., 2003). Furthermore, this would result in a much more pronounced isotopic minimum in the granites (down to values as low as  $-60\%$ ) and the shape of the diffusion profile in the syenite would be different from what is observed ( $\delta^7\text{Li}$  should peak well into the body and not at the chilled margin). Thus, whereas diffusive infiltration from the syenite to the granite country rock can explain the isotopic minimum and its position within the granites, it cannot reproduce the very heavy Li isotopic compositions found in the outermost augite syenite samples and the peak  $\delta^7\text{Li}$  at the chilled margin. Consequently, additional processes must have influenced the isotopic composition of the syenite.

High  $\delta^7\text{Li}$  values may also result from interaction between magmas and aqueous fluids, since the latter tend to concentrate the heavy isotope (e.g., Teng et al., 2006b). The fluid phase could be either internally or externally derived. Since amphiboles that crystallized from the late Ilímaussaq fluids have  $\delta^7\text{Li}$  values between +2 and +5 (see above), a purely internally derived fluid source seems unlikely to explain the significantly heavier isotopic compositions found in the outer parts of the augite syenite. Late-stage fluid circulation within the augite syenite is evident from analcite–sodalite–hydrogrossular assemblages found in some samples, reflecting hydrothermal alteration at  $\approx 400$  °C (Marks and Markl, 2001; Markl et al., 2001). Moreover, the occurrence of aegirine-rich veins within the country rock granite up to 250 m away from the Ilímaussaq complex is evidence for the circulation of alkaline fluids well outside the Ilímaussaq complex. The distinctly higher  $\delta^7\text{Li}$  and low  $\delta^{18}\text{O}$  value of pyroxene from this aegirine-rich vein compared to other late-stage samples is consistent with a meteoric origin (see above) and thus implies that mixing between alkaline Ilímaussaq fluids and fluids from external sources (e.g., groundwater, saline lake water or seawater) has occurred. The existence of two distinct fluid phases can also be inferred from the hydrogen isotopic disequilibrium between biotite and amphibole in augite syenite samples (see above). Calculated  $\delta D$  values for the fluid phase co-existing with late-stage biotite approach zero, for temperatures  $< 400$  °C (using the calibration of Suzuoki and Epstein, 1976), suggesting the possibility of an ingress of seawater during final cooling of these rocks. When taking into account the variation in chemical composition of the biotites (which influences the fractionation of hydrogen isotopes between mica and water) the inferred isotopic influence of seawater increases towards the margin of the augite syenite unit.

In summary, we propose a two-stage model, where, in addition to the diffusional processes discussed above, the ingress of an external fluid phase having higher  $\delta^7\text{Li}$  and  $\delta D$  than the augite syenite shifted the outer regions of the augite syenite unit to higher  $^7\text{Li}$  and  $\delta D$  values. This effect was most pronounced in the outermost part of the augite syenite unit and may result from a greater amount of fracturing (hence porosity) compared to country rock granites, as is evident from the field. Given the high  $\delta^7\text{Li}$  value of seawater (around +31‰; Millot et al., 2004), basinal brines (Bottomley et al., 1999, 2003) and saline lake water (+17 to +34‰, Tomascak et al., 2003, and references therein) and the relatively high  $\delta D$  values of biotites in the augite syenite (see

above; Table 2a) it seems reasonable that such waters could potentially be the source of the heavy Li. Infiltration of such waters is also consistent with this magmatism occurring in a continental rift setting (cf. East African rift or Red Sea).

[Li] in present-day seawater is <0.2 ppm (Bruland & Lohan, 2004) and ranges from <0.2 to 15 ppm in saline lakes (Tomascak et al., 2003). Given this and the high solubility and mobility of Li in fluids, large amounts of circulating saline waters may have leached Li from the rock and could thus explain the low [Li] of this unit ( $\leq 25$  ppm) relative to the other units ( $>100$  ppm; Table 3). Assuming a minimum  $D_{\text{cpx-melt}}^{\text{Li}}$  of  $\sim 0.14$  (Brenan et al., 1998a) and using the lowest [Li] of cpx measured in the augite syenite unit (14 ppm; Table 2a) yields a minimum [Li] in the augite syenite melt of  $\sim 100$  ppm, compared to the highest measured [Li] of 25 ppm. The exceptionally low [Li] of only 7 ppm in the outermost sample is far too low to represent a magmatic value for such a highly fractionated syenitic magma (e.g., Bailey et al., 2001).

It is also interesting to note that intra-mineral Li isotope fractionations in the augite syenite samples vary greatly (Tables 2a and 2b; Fig. 3) and the expected order of fractionation (see above) is preserved only in the two outermost samples (GM1858 & GM1330), whereas this order is disturbed in the three inner samples. Minerals of these two outermost samples obviously re-equilibrated with an isotopically heavy Li source, while samples more distant to this zone did not.

## 7. Summary and conclusions

The incorporation of Li into amphiboles is mainly influenced by changes in their major element composition and by changes in oxygen fugacity during magmatic differentiation. Changing mineral compositions can account for the high Li concentrations in Na-amphiboles ( $>360$  ppm) compared to Ca-amphiboles ( $<70$  ppm). In Na-amphiboles, Li concentrations correlate with  $\text{Fe}^{3+}/\Sigma\text{Fe}$  ratios, implying that oxygen fugacity influences the incorporation of Li into the amphibole structure due to charge balance constraints. Clinopyroxenes do not show a similar correlation, which can be explained by different site preferences for Li in the amphibole and clinopyroxene structures. This observation raises the possibility that relative changes of Li concentrations in Na-amphiboles could be used as a qualitative oxybarometer in peralkaline magmatic systems undergoing differentiation.

The Li isotopic compositions ( $\delta^7\text{Li}$ ) of all minerals (amphiboles and pyroxenes) span a wide range from

+17 to  $-8\%$ . Homogeneous  $\delta^7\text{Li}$  values of amphiboles from the inner part of the complex (mean value of  $+1.8 \pm 2.2\%$ ,  $2\sigma$ ) likely reflect the  $\delta^7\text{Li}$  of the mantle source of the parental melt and imply a lack of Li isotopic fractionation during magmatic differentiation and fluid exsolution. In contrast, samples from the outermost part of the complex have large and spatially systematic Li isotope and concentration variations. This, coupled with the Li systematics of country rock granites adjacent to this unit, is clear evidence for post-magmatic open-system processes occurring during final cooling of these rocks. We suggest a two-step model where, in addition to fluid infiltration and diffusion from the augite syenite into the country rock granite, significant ingress and circulation of a fluid rich in  $^7\text{Li}$  (e.g., seawater or saline lake water) occurred along the chilled margin of the augite syenite. This demonstrates the suitability of the Li isotope system to decipher such fluid- and diffusion-governed processes.

## Acknowledgments

Financial support for this work was granted by the Deutsche Forschungsgemeinschaft (grant Ma2563/2-1) and NSF grants EAR0208012 and EAR 0609689. M.M. especially thanks Alevtina Dorn for the careful and time-consuming hand picking of the large number of mineral separates used in this study and Melanie Kaliwoda for making available unpublished data on Li concentrations of minerals and whole-rocks from Ilimaussaq. Elena Chung, Fang-Zhen Teng, Ralf Halama, Bill McDonough, Igor Puchtel, Jeffrey Ryan and Richard Ash are thanked for their valuable help during the analytical work in College Park, Maryland. Florian Neukirchen is thanked for his assistance during fieldwork 2006. Babette Förch helped to improve an earlier version of the manuscript and M.M. thanks her for being a great enrichment to his life. Thomas Zack, Fang-Zhen Teng, Ralf Halama, Chris Harris, Boswell Wing, James Farquar, Jay Ague and Sash Heir-Majumder provided fruitful discussions on various aspects of this work and Volker Presser is thanked for support during the modeling calculations. The constructive comments of P. Tomascak, B. Leeman and one anonymous reviewer are greatly appreciated.

## References

- Audétat, A., Pettke, T., 2003. The magmatic-hydrothermal evolution of two barren granites: a melt and fluid inclusion study of the Rito del Medio and Canada Pinabete plutons in northern New Mexico (USA). *Geochimica et Cosmochimica Acta* 67, 97–121.

- Badanina, E.V., Veskler, I.V., Thomas, R., Syritso, L.F., Trumbull, R.B., 2004. Magmatic evolution of Li–F, rare-metal granites: a case study of melt inclusions in the Khangilay complex, Eastern Transbaikalia (Russia). *Chemical Geology* 210, 113–133.
- Bailey, J.C., Gwodzi, R., 1994. Li distribution in aegirine lujavrite, Ilímaussaq alkaline intrusion, South Greenland: role of cumulus and post-cumulus processes. *Lithos* 31, 207–225.
- Bailey, J.C., Bohse, H., Gwodzi, R., Rose-Hansen, J., 1993. Li in minerals from the Ilímaussaq alkaline intrusion, South Greenland. *Bulletin of the Geological Society of Denmark* 40, 288–299.
- Bailey, J.C., Gwodzi, R., Rose-Hansen, J., Sørensen, H., 2001. Geochemical overview of the Ilímaussaq alkaline complex, South Greenland. *Geology of Greenland Survey Bulletin* 190, 35–53.
- Barrat, J.A., Chaussidon, M., Bohn, M., Gillet, Ph., Göpel, C., Lesourd, M., 2005. Lithium behavior during cooling of a dry basalt: an ion-microprobe study of the lunar meteorite Northwest Africa 479 (NWA 479). *Geochimica et Cosmochimica Acta* 69, 5597–5609.
- Beck, P., Chaussidon, M., Barrat, J.A., Gillet, P., Bohn, M., 2006. Diffusion induced Li isotopic fractionation during the cooling of magmatic rocks: the case of pyroxene phenocrysts from nakhlite meteorites. *Geochimica et Cosmochimica Acta* 70, 4813–4825.
- Benton, L.D., Ryan, C.G., Savov, I.P., 2004. Lithium abundances and isotope systematics of forearc serpentinites, Conical Seamount, Mariana forearc: insights into the mechanics of slab–mantle exchange during subduction. *Geochemistry Geophysics Geosystems* 5. doi:10.1029/2004GC000708.
- Berger, G., Schott, J., Guy, C., 1988. Behavior of Li, Rb and Cs during basalt glass and olivine dissolution and chlorite, smectite and zeolite precipitation from seawater-experimental investigations and modelization between 50 °C and 300 °C. *Chemical Geology* 71, 297–312.
- Blaxland, A.B., 1976. Age and origin of apgaitic magmatism at Ilímaussaq, South Greenland: Rb–Sr study. *Lithos* 9, 31–38.
- Bottomley, D.J., Katz, A., Chan, L.H., Starinsky, A., Douglas, M., Clark, I.D., Raven, K.G., 1999. The origin and evolution of Canadian shield brines: evaporation or freezing of seawater? New lithium isotope and geochemical evidence from the Slave craton. *Chemical Geology* 155, 295–320.
- Bottomley, D.J., Chan, L.H., Katz, A., Starinsky, A., Clark, I.D., 2003. Lithium isotope geochemistry and origin of Canadian shield brines. *Groundwater* 41, 847–856.
- Bouman, C., Elliott, T., Vroon, P.Z., 2004. Lithium inputs to subduction zones. *Chemical Geology* 212, 59–79.
- Brenan, J.M., Neroda, E., Lundstrom, C.C., Shaw, H.F., Ryerson, F.J., Phinney, D.L., 1998a. Behaviour of boron, beryllium, and lithium during melting and crystallization: constraints from mineral–melt partitioning experiments. *Geochimica et Cosmochimica Acta* 62, 2129–2141.
- Brenan, J.M., Ryerson, F.J., Shaw, H.F., 1998b. The role of aqueous fluids in the slab-to-mantle transfer of boron, beryllium, and lithium during subduction: experiments and models. *Geochimica et Cosmochimica Acta* 62, 3337–3347.
- Bruland, K.W., Lohan, M.C., 2004. Controls of trace metals in seawater. *Treatise on Geochemistry* 6, 23–48.
- Bryant, C.J., Chappell, B.W., Bennet, V.C., McCulloch, M.T., 2004. Lithium isotopic composition of the New England Batholith: correlations with inferred source rock compositions. *Transactions of the Royal Society of Edinburgh. Earth Sciences* 95, 199–214.
- Cartwright, I., Valley, J.W., 1991. Steep oxygen-isotope gradients at marble–metagranite contacts in the northwest Adirondack Mountains, New York, USA: products of fluid-hosted diffusion. *Earth and Planetary Science Letters* 107, 148–163.
- Cerny, P., Masau, M., Goad, B.E., Ferreira, K., 2005. The Greer Lake leucogranites, Manitoba, and the origin of lepidolite-subtype granitic pegmatites. *Lithos* 80, 305–321.
- Chan, L.-H., Frey, F.A., 2003. Lithium isotope geochemistry of the Hawaiian plume: results from the Hawaiian Scientific Drilling Project and Koolau Volcano. *Geochemistry Geophysics Geosystems* 4, 8707.
- Chan, L.H., Edmond, J.M., Thompson, G., Gillis, K., 1992. Lithium isotopic composition of submarine basalts: implications for the lithium cycle in the oceans. *Earth and Planetary Science Letters* 108, 151–160.
- Chan, L.H., Gieskes, J.M., You, C.F., Edmond, J.M., 1994. Lithium isotope geochemistry of sediments and hydrothermal fluids of the Guaymas Basin, gulf of California. *Geochimica et Cosmochimica Acta* 58, 4443–4454.
- Chan, L.H., Leeman, W.P., You, C.-F., 2002. Lithium isotopic composition of Central American Volcanic Arc lavas: implications for modification of subarc mantle by slab-derived fluids: corrections. *Chemical Geology* 182, 293–300.
- Clayton, R.N., Mayeda, T.K., 1963. The use of bromine pentafluoride in the extraction of oxygen from oxides and silicates for isotope analysis. *Geochimica et Cosmochimica Acta* 43–52.
- Coogan, L.A., Kasemann, S.A., Chakraborty, S., 2005. Rates of hydrothermal cooling of new oceanic upper crust derived from lithium-geospeedometry. *Earth and Planetary Science Letters* 240, 415–424.
- Crank, J., 1975. *The Mathematics of Diffusion*. Oxford University Press, Oxford, p. 414.
- Decitre, S., Deloule, E., Reisberg, L., James, R.H., Agrinier, P., Mével, C., 2002. Behavior of Li and its isotopes during serpentinization of oceanic peridotites. *Geochemistry Geophysics Geosystems* 3.
- Della Ventura, G., Iezzi, G., Redhammer, G.J., Hawthorne, F.C., Scaillet, B., Novembre, D., 2005. Synthesis and crystal-chemistry of alkali amphiboles in the system Na<sub>2</sub>O–MgO–FeO–Fe<sub>2</sub>O<sub>3</sub>–SiO<sub>2</sub>–H<sub>2</sub>O as a function of *f*<sub>O<sub>2</sub></sub>. *American Mineralogist* 90, 1375–1383.
- Edgar, A.D., Parker, L.M., 1974. Comparison of melting relationships of some plutonic and volcanic peralkaline undersaturated rocks. *Lithos* 7, 263–273.
- Elliott, T., Thomas, A., Jeffcoate, A., Niu, Y.L., 2006. Lithium isotope evidence for subduction-enriched mantle in the source of mid-ocean-ridge basalts. *Nature* 443, 565–568.
- Enders, M., Speer, D., Maresch, W.V., McCammon, C., 2000. Ferric/ferrous iron ratios in sodic amphiboles: Mössbauer analysis, stoichiometry-based model calculations and the high-resolution microanalytical flank method. *Contributions to Mineralogy and Petrology* 140, 135–147.
- Engell, J., Hansen, J., Jensen, M., Kunzendorf, H., Løvborg, L., 1971. Beryllium mineralization in the Ilímaussaq Intrusion, South Greenland, with description of a field beryllometer and chemical methods. *Rapport Grønlands Geologiske Undersøgelse* 33, 40.
- Farver, J.R., 1989. Oxygen self-diffusion in diopside with applications to cooling rate determinations. *Earth and Planetary Science Letters* 92, 386–396.
- Farver, J.R., Giletti, B.J., 1985. Oxygen diffusion in amphiboles. *Geochimica Cosmochimica Acta* 49, 1403–1411.
- Ferguson, J., 1964. *Geology of the Ilímaussaq alkaline intrusion, South Greenland. Bulletin Grønlands Geologiske Undersøgelse* 39, 82.
- Flesch, G.D., Anderson, A.R., Svec, H.J., 1973. A secondary isotopic standard for <sup>6</sup>Li/<sup>7</sup>Li determinations. *International Journal of Mass Spectrometry and Ion Processes* 12, 265–272.
- Foustoukos, D.I., James, R.H., Berndt, M.E., Seyfried, W.E.J., 2004. Lithium isotopic systematics of hydrothermal vent fluids at the

- Main Endeavour Field, Northern Juan de Fuca Ridge. *Chemical Geology* 212, 17–26.
- Fritz, S.J., 1992. Measuring the ratio of aqueous diffusion coefficients between  $^6\text{LiCl}$  and  $^7\text{LiCl}$  by osmometry. *Geochimica et Cosmochimica Acta* 56, 3781–3789.
- Garde, A.A., Hamilton, M.A., Chadwick, B., Grocott, J., McCaffrey, K.J.W., 2002. The Ketilidian orogen of South Greenland: geochronology, tectonics, magmatism, and fore-arc accretion during Palaeoproterozoic oblique convergence. *Canadian Journal of Earth Sciences* 39, 765–793.
- Giletti, B.J., Shanahan, T.M., 1997. Alkali diffusion in plagioclase feldspar. *Chemical Geology* 139, 3–20.
- Govindaraju, B., 1989. Compilation of working values and sample description for 272 geostandards. *Geostandards Newsletter* 13, 1–113.
- Graser G., and Markl G. (in revision) Ilvaite–epidote–hydrogarnet endoskarns record late-magmatic fluid influx into the peridotite Ilimaussaq complex, South Greenland. *Journal of Petrology*.
- Halama, R., Wenzel, T., Upton, B.G.J., Siebel, W., Markl, G., 2003. A geochemical and Sr–Nd–O isotopic study of the Proterozoic Eriksfjord Basalts, Gardar Province, South Greenland: reconstruction of an OIB-signature in crustally contaminated rift-related basalts. *Mineralogical Magazine* 67, 831–853.
- Halama, R., Marks, M., Brüggemann, G., Siebel, W., Wenzel, T., Markl, G., 2004. Crustal contamination of mafic magmas: evidence from a petrological, geochemical and Sr–Nd–Os–O isotopic study of the Proterozoic Isortoq dike swarm, South Greenland. *Lithos* 74, 199–232.
- Halama, R., McDonough, W.F., Rudnick, R.L., Keller, J., Klaudius, J., 2007. The Li isotopic composition of Oldoinyo Lengai: nature of the mantle sources and lack of isotopic fractionation during carbonatite genesis. *Earth and Planetary Science Letters* 254, 77–89.
- Halama R., McDonough W.F., Rudnick R.L., Bell K. (in revision). Tracking the lithium isotopic evolution of the mantle using carbonatites. *EPSL*.
- Hawthorne, F.C., Ungaretti, L., Oberti, R., Cannillo, E., 1994. The mechanisms of [6] Li incorporation in amphiboles. *American Mineralogist* 79, 443–451.
- Huh, Y., Chan, L.-H., Zhang, L., Edmond, J.M., 1998. Lithium and its isotopes in major world rivers: Implications for weathering and the oceanic budget. *Geochimica et Cosmochimica Acta* 62, 2039–2051.
- Huh, Y., Chan, L.-H., Edmond, J.M., 2001. Lithium isotopes as a probe of weathering processes: Orinoco river. *Earth and Planetary Science Letters* 194, 189–199.
- James, R.H., Allen, D.E., Seyfried, W.E.J., 2003. An experimental study of alteration of oceanic crust and terrigenous sediments at moderate temperatures (51 to 350 °C): insights as to chemical processes in near-shore ridge-flank hydrothermal systems. *Geochimica et Cosmochimica Acta* 67, 681–691.
- Jeffcoate, A.B., Elliott, T., Thomas, A., Bouman, C., 2004. Precise, small sample size determination of lithium isotope compositions of geological reference materials and modern seawater by MC-ICP-MS. *Geostandards Newsletter* 28, 161–172.
- Jeffcoate, A., Elliot, T., Kasemann, S.A., Ionov, D.A., Cooper, K.M., Brooker, R.A., 2007. Lithium isotope fractionation in peridotites and mafic melts. *Geochimica et Cosmochimica Acta* 71, 202–218.
- Kaliwoda, M., Altherr, R., Markl, G., 2007. Li, Be, B and  $\delta^{11}\text{B}$  values from the peralkaline Ilimaussaq intrusion and its country rocks (South Greenland). *Geochimica et Cosmochimica Acta* 71 (15S), A459.
- Kalsbeek, F., Taylor, P.N., 1985. Isotopic and chemical variation in granites across a Proterozoic continental margin—the Ketilidian mobile belt of South Greenland. *Earth and Planetary Science Letters* 73, 65–80.
- Khomyakov, A.P., 1995. Mineralogy of hyperagpaite alkaline rocks. Clarendon Press, Oxford, p. 222. Oxford Scientific Publications.
- Kogarko, L.N., 1977. General regularities of differentiation of magmas oversaturated with alkalis. *Geochemistry International* 14, 9–25.
- Kogarko, L.N., Romanev, B.P., 1977. Temperature, pressure, redox conditions, and mineral equilibria in agpaite nepheline syenites and apatite-nepheline rocks. *Geochemistry International* 14, 113–128.
- Konnerup-Madsen, J., 2001. A review of the composition and evolution of hydrocarbon gases during solidification of the Ilimaussaq alkaline complex, South Greenland. *Geology of Greenland Survey Bulletin* 190, 159–166.
- Krumrei, T.V., Villa, I.M., Marks, M.A.W., Markl, G., 2006. A  $^{40}\text{Ar}/^{39}\text{Ar}$  and U/Pb isotopic study of the Ilimaussaq complex, South Greenland: implications for the  $^{40}\text{K}$  decay constant and for the duration of magmatic activity in a peralkaline complex. *Chemical Geology* 227, 258–273.
- Krumrei, T.V., Pernicka, E., Kaliwoda, M., Markl, G., 2007. Volatiles in a peralkaline system: abiogenic hydrocarbons and F–Cl–Br systematics in the naujaite of the Ilimaussaq intrusion, South Greenland. *Lithos* 95, 298–314.
- Larsen, L.M., 1976. Clinopyroxenes and coexisting mafic minerals from the alkaline Ilimaussaq intrusion, south Greenland. *Journal of Petrology* 17, 258–290.
- Larsen, L.M., Sørensen, H., 1987. The Ilimaussaq intrusion—progressive crystallization and formation of layering in an agpaite magma. In: Fitton, J.G., Upton, B.G.J. (Eds.), *Alkaline igneous rocks*, vol. 30. Geological Society of London, pp. 473–488 (Special Publication).
- Li, Y.-H., Gregory, S., 1974. Diffusion of ions in sea water and in deep-sea sediments. *Geochimica et Cosmochimica Acta* 38, 703–714.
- Lundstrom, C.C., Chaussidon, M., Hsui, A.T., Kelemen, P.B., Zimmermann, M., 2005. Observations of Li isotopic variations in the Trinity Ophiolite: evidence for isotopic fractionation by diffusion during mantle melting. *Geochimica et Cosmochimica Acta* 69, 735–751.
- Lynton, S.L., Walker, R.J., Candela, P.A., 2005. Lithium isotopes in the system Qz–Ms–fluid: an experimental study. *Geochimica et Cosmochimica Acta* 69, 3337–3347.
- Magna, T., Wiechert, U.H., Halliday, A.N., 2004. Low-blank isotope ratio measurement of small samples of lithium using multiple-collector ICPMS. *International Journal of Mass Spectrometry* 239, 67–76.
- Magna, T., Wiechert, U., Grove, T.L., Halliday, A.N., 2006. Lithium isotope fractionation in the southern Cascadia subduction zone. *Earth and Planetary Science Letters* 250, 428–443.
- Markl, G., 2001. A new type of silicate liquid immiscibility in peralkaline nepheline syenites (lujavrites) of the Ilimaussaq complex, South Greenland. *Contributions to Mineralogy and Petrology* 141, 458–472.
- Markl, G., Baumgartner, L., 2002. pH changes in peralkaline late-magmatic fluids. *Contributions to Mineralogy and Petrology* 144, 331–346.
- Markl, G., Marks, M., Schwinn, G., Sommer, H., 2001. Phase equilibrium constraints on intensive crystallization parameters of the Ilimaussaq Complex, South Greenland. *Journal of Petrology* 42, 2231–2258.
- Marks, M., Markl, G., 2001. Fractionation and assimilation processes in the alkaline augite syenite unit of the Ilimaussaq Intrusion,

- South Greenland, as deduced from phase equilibria. *Journal of Petrology* 42, 1947–1969.
- Marks, M., Vennemann, T., Siebel, W., Markl, G., 2003. Quantification of magmatic and hydrothermal processes in a peralkaline syenite-alkali granite complex based on textures, phase equilibria, and stable and radiogenic isotopes. *Journal of Petrology* 44, 1247–1280.
- Marks, M., Vennemann, T., Siebel, W., Markl, G., 2004. Nd-, O-, and H-isotopic evidence for complex, closed-system fluid evolution of the peralkaline Ilímaussaq Intrusion, South Greenland. *Geochimica et Cosmochimica Acta* 68, 3379–3395.
- McCammom, C.A., 2004. Mössbauer spectroscopy: applications. In: Beran, A., Libowitzky, E. (Eds.), *Spectroscopic Methods in Mineralogy*, vol. 6. Eötvös University Press, pp. 369–398.
- Mengel, K., 1990. Crustal xenoliths from Tertiary volcanics of the northern Hessian depression. *Petrological and chemical evolution. Contributions to Mineralogy and Petrology* 104, 8–26.
- Millot, R., Guerrot, C., Vigier, N., 2004. Accurate and high-precision measurements of lithium isotopes in two reference materials. *Geostandards and Geoanalytical Research* 28, 153–159.
- Moriguti, T., Nakamura, E., 1998. High-yield lithium separation and the precise isotopic analysis of natural rock and aqueous samples. *Chemical Geology* 145, 91–104.
- Parkinson I.J., Hammond S.J., James R.H., Rogers N.W., 2007. High-temperature lithium isotope fractionation: Insights from lithium isotope diffusion in magmatic systems. *Earth and Planetary Science Letters* 257, 609–621.
- Pistiner, J.S., Henderson, G.M., 2003. Lithium-isotope fractionation during continental weathering process. *Earth and Planetary Science Letters* 214, 327–339.
- Poulsen, V., 1964. The sandstones of the Precambrian Eriksfjord Formation in South Greenland. *Rapport Grønlands Geologiske Undersøgelse* 2, 16.
- Ranlov, J., Dymek, F., 1991. Compositional zoning in hydrothermal aegirine from fenites in the Proterozoic Gardar Province, South Greenland. *European Journal of Mineralogy* 3, 837–853.
- Redhammer, G.J., Roth, G., Paulus, W., André, G., Lottermoser, W., Amthauer, G., Treutmann, W., Koppelhuber-Bitschnau, B., 2001. The crystal and magnetic structure of Li-aegirine  $\text{LiFe}_3+\text{Si}_2\text{O}_6$ : a temperature-dependent study. *Physics and Chemistry of Minerals* 28, 337–346.
- Richter, F.M., Liang, Y., Davis, A.M., 1999. Isotope fractionation by diffusion in molten oxides. *Geochimica et Cosmochimica Acta* 63, 2853–2861.
- Richter, F.M., Davis, A.M., DePaolo, D., Watson, E.B., 2003. Isotope fractionation by chemical diffusion between molten basalt and rhyolite. *Geochimica et Cosmochimica Acta* 67, 3905–3923.
- Romer, R.L., Heinrich, W., Schröder-Smeibidl, B., Meixner, A., Fischer, C.-O., Schulz, C., 2005. Elemental dispersion and stable isotope fractionation during reactive fluid-flow and fluid immiscibility in the Buf del Diente aureole, NE-Mexico: evidence from radiographies and Li, B, Sr, Nd, and Pb isotope systematics. *Contributions to Mineralogy and Petrology* 149, 400–429.
- Rudnick R., Gao S. (2003) Composition of the continental crust. in: Rudnick, R. (ed.), *The Crust*, Vol. 3 of *Treatise on geochemistry* (eds. H.D. Holland & K.K. Turekian), Elsevier–Pergamon, Oxford.
- Rudnick, R., Ionov, D.A., 2007. Lithium elemental and isotopic disequilibrium in minerals from peridotite xenoliths from far-east Russia: product of recent melt/fluid–rock interaction. *Earth and Planetary Science Letters* 256, 278–293.
- Rudnick, R., Nakamura, E., 2004. Preface to “lithium isotope geochemistry”. *Chemical Geology* 212, 1–4.
- Rudnick, R., Tomascak, P.B., Njo, H.B., Gardner, L.R., 2004. Extreme lithium isotopic fractionation during continental weathering revealed in saprolites from South Carolina. *Chemical Geology* 212, 45–57.
- Rumble, D., Hoering, T.C., 1994. Analysis of oxygen and sulfur isotope ratios in oxide and sulfide minerals by spot heating with a carbon dioxide laser in a fluorine atmosphere. *Accounts of Chemical Research* 27, 237–241.
- Ryan, J.G., Kyle, P.R., 2004. Lithium abundance and lithium isotope variations in mantle sources: insights from intraplate volcanic rocks from Ross Island and Marie Byrd Land (Antarctica) and other oceanic island. *Chemical Geology* 212, 125–142.
- Ryan, J.G., Langmuir, C.H., 1987. The systematics of lithium abundances in young volcanic rocks. *Geochimica et Cosmochimica Acta* 51, 1727–1741.
- Schauble, E.A., 2004. Applying stable isotope fractionation theory to new systems. in: Johnson, C.M., Beards, B.I., Albarede, F. (eds.), *Geochemistry of Non-Traditional Isotopes: Reviews in Mineralogy and Geochemistry*, vol. 55, pp. 65–111.
- Schmitt, A.K., Emmermann, R., Trumbull, R.B., Bühn, B., Henjes-Kunst, F., 2000. Petrogenesis and  $^{40}\text{Ar}/^{39}\text{Ar}$  geochronology of the Brandberg Complex, Namibia: evidence for a major mantle contribution in metaluminous and peralkaline granites. *Journal of Petrology* 41, 1207–1239.
- Seyfried, W.E.J., Chen, X., Chan, L.H., 1998. Trace element mobility and lithium isotope exchange during hydrothermal alteration of seafloor weathered basalt: an experimental study at 350 °C, 500 bars. *Geochimica et Cosmochimica Acta* 62, 949–960.
- Sharp, Z.D., 1990. A laser-based microanalytical method for the in-situ determination of oxygen isotope ratios of silicates and oxides. *Geochimica et Cosmochimica Acta* 54, 1353–1357.
- Sharp, Z.D., Atudorei, V., Durakiewicz, T., 2001. A rapid method for determining the hydrogen and oxygen isotope ratios from water and solid hydrous substances. *Chemical Geology* 178, 197–210.
- Sood, M.K., Edgar, A.D., 1970. Melting relations of undersaturated alkaline rocks. *Meddelelser om Grønland* 181, 41.
- Sørensen, H., 1997. The apatitic rocks—an overview. *Mineralogical Magazine* 61, 485–498.
- Sørensen, H., 2001. Brief introduction to the geology of the Ilímaussaq alkaline complex, South Greenland. *Geology of Greenland Survey Bulletin* 190, 7–24.
- Sørensen, H., 2006. The origin and mode of emplacement of lujavrites in the Ilímaussaq alkaline complex, south Greenland. *Lithos* 91, 286–300.
- Stevenson, R., Upton, B.G.J., Steenfelt, A., 1997. Crust–mantle interaction in the evolution of the Ilímaussaq Complex, South Greenland: Nd isotopic studies. *Lithos* 40, 189–202.
- Suzuoki, T., Epstein, S., 1976. Hydrogen isotope fractionation between OH-bearing minerals and water. *Geochimica et Cosmochimica Acta* 40, 1229–1240.
- Taylor, B.E., 1986. Magmatic volatiles: isotopic variation of C, H, and S. *Reviews in Mineralogy* 16, 185–226.
- Taylor, I.T., Urey, H.C., 1938. Fractionation of lithium and potassium isotopes by chemical exchange with zeolithe. *Journal of Chemical Physics* 6, 429–439.
- Teng, F.-Z., McDonough, W.F., Rudnick, R.L., Dalpé, C., Tomascak, P.B., Chappell, B.W., Gao, S., 2004a. Lithium isotopic composition and concentration of the upper continental crust. *Geochimica et Cosmochimica Acta* 68, 4167–4178.
- Teng, F.-Z., McDonough, W.F., Rudnick, R.L., Gao, S., 2004b. Lithium isotopic composition of the deep continental crust. *EOS* 85, V51C–0597.

- Teng, F.-Z., McDonough, W.F., Rudnick, R.L., Walker, R.J., Sirbescu, M.-L.C., 2006a. Lithium isotopic systematics of granites and pegmatites from the Black Hills, South Dakota. *American Mineralogist* 91, 1488–1498.
- Teng, F.-Z., McDonough, W.F., Rudnick, R.L., Walker, R.J., 2006b. Diffusion driven extreme lithium isotopic fractionation in country rocks of the Tin Mountain pegmatite. *Earth and Planetary Science Letters* 243, 701–710.
- Teng, F., Rudnick, R.L., McDonough, W.F., Tomascak P.B., submitted for publication. Lithium isotopic composition and concentration of the deep continental crust.
- Thompson, R.M., Downs, R.T., 2003. Model pyroxenes I: Ideal pyroxene topologies. *American Mineralogist* 88, 653–666.
- Tomascak, P.B., 2004. Developments in the understanding and application of lithium isotopes in the Earth and planetary sciences. *Reviews in Mineralogy* 55, 153–196.
- Tomascak, P.B., Tera, F., Helz, R.T., Walker, R.J., 1999a. The absence of lithium isotope fractionation during basalt differentiation: new measurements by multicollector sector ICP-MS. *et Cosmochimica Acta* 63, 907–910.
- Tomascak, P.B., Carlson, R.W., Shirey, S.B., 1999b. Accurate and precise determination of Li isotopic compositions by multicollector ICP-MS. *Chemical Geology* 158, 145–154.
- Tomascak, P.B., Ryan, J.G., Defant, M.J., 2000. Lithium isotope evidence for light element decoupling in the Panama subarc mantle. *Geology* 28, 507–510.
- Tomascak, P.B., Widom, E., Benton, L.D., Goldstein, S.L., Ryan, J.G., 2002. The control of lithium budgets in island arcs. *Earth and Planetary Science Letters* 196, 227–238.
- Tomascak, P.B., Hemming, N.G., Hemming, S.R., 2003. The lithium isotopic composition of waters of the Mono Basin, California. *Geochimica et Cosmochimica Acta* 67, 601–611.
- Tomascak P.B., Langmuir C.H., le Roux P.J., Shirey S.B., in revision. Lithium isotopes in global mid-ocean ridge basalts. *Geochimica et Cosmochimica Acta*.
- Tuttle, O.F., Bowen, N.L., 1958. Origin of granite in the light of experimental studies in the system  $\text{NaAlSi}_3\text{O}_8$ – $\text{KAlSi}_3\text{O}_8$ – $\text{SiO}_2$ – $\text{H}_2\text{O}$ . *Memoirs of the Geological Society of America* 74.
- Valley, J.W., Kitchen, N., Kohn, M.J., Niendorf, C.R., Spicuzza, M.J., 1995. UWG-2, a garnet standard for oxygen isotope ratios: strategies for high precision and accuracy with laser heating. *Geochimica et Cosmochimica Acta* 59, 5223–5231.
- Van Alboom, A., De Grave, E., 1996. Temperature dependence of the  $^{57}\text{Fe}$  Mössbauer parameters in riebeckite. *Physics and Chemistry of Minerals* 23, 377–386.
- Vennemann, T.W., O'Neil, J.R., 1993. A simple and inexpensive method of hydrogen isotope and water analyses of minerals and rocks based on zinc reagent. *Geology* 103, 227–234.
- Vennemann, T.W., Smith, H.S., 1991. The rate and temperature of reaction of  $\text{ClF}_3$  with silicate minerals, and their relevance to oxygen isotope analysis. *Chemical Geology* 86, 83–88.
- Wunder, B., Meixner, A., Romer, R.L., Heinrich, W., 2006. Temperature-dependent isotopic fractionation of lithium between clinopyroxene and high-pressure hydrous fluids. *Contributions to Mineralogy and Petrology* 151, 112–120.
- Wunder B., Meixner A., Romer R.L., Feenstra A., Schettler G., Heinrich W., 2007. Lithium isotope fractionation between Li-bearing staurolite, Li-mica and aqueous fluids: An experimental study. *Chemical Geology* 238, 277–290.
- You, C.F., Chan, L.H., 1996. Precise determination of lithium isotopic composition in low concentration natural samples. *Geochimica et Cosmochimica Acta* 60, 909–915.
- You, C.F., Morris, J.D., Gieskes, J.M., Rosenbauer, R., Zheng, S.H., Xu, X., Ku, T.L., Bischoff, J.L., 1994. Mobilization of Be in sedimentary column at convergent margins. *Geochimica et Cosmochimica Acta* 58, 4887–4897.
- Zack, T., Tomascak, P.B., Rudnick, R.L., Dalpé, C., McDonough, W.F., 2003. Extremely light Li in orogenic eclogites: the role of isotope fractionation during dehydration in subducted oceanic crust. *Earth and Planetary Science Letters* 208, 279–290.
- Zhang, L., Chan, L.H., Gieskes, J.M., 1998. Lithium isotope geochemistry of pore waters from Ocean Drilling Program Sites 918 and 919, Irminger Basin. *Geochimica et Cosmochimica Acta* 62, 2437–2450.
- Zheng, Y.-F., 1993a. Calculation of oxygen isotope fractionation in anhydrous silicates. *Geochimica et Cosmochimica Acta* 57, 1079–1091.
- Zheng, Y.-F., 1993b. Calculation of oxygen isotope fractionation in hydroxyl-bearing silicates. *Earth and Planetary Science Letters* 120, 247–263.